Arabian Journal of Chemistry (2018) xxx, xxx–xxx

King Saud University

Arabian Journal of Chemistry

www.ksu.edu.sa
www.sciencedirect.com

REVIEW ARTICLE

A review on the classification of organic/inorganic/carbonaceous hole transporting materials for perovskite solar cell application

Selvakumar Pitchaiya [a,*], Muthukumarasamy Natarajan [a,*], Agilan Santhanam [a], Vijayshankar Asokan [b], Akila Yuvapragasam [a], Venkatraman Madurai Ramakrishnan [a], Subramaniam E. Palanisamy [c], Senthilarasu Sundaram [d], Dhayalan Velauthapillai [e]

[a] *Department of Physics, Coimbatore Institute of Technology, Coimbatore, Tamil Nadu, India*
[b] *Environmental Inorganic Chemistry, Department of Chemistry and Chemical Engineering, Chalmers University of Technology, 412 96 Göteborg, Sweden*
[c] *Department of Chemistry, Coimbatore Institute of Technology, Coimbatore, Tamil Nadu, India*
[d] *Environment and Sustainability Institute, University of Exeter, Penryn, Cornwall TR10 9FE, United Kingdom*
[e] *Faculty of Engineering and Science, Western Norway University of Applied Sciences, 5063 Bergen, Norway*

Received 19 February 2018; accepted 18 June 2018

KEYWORDS

Perovskite solar cells;
Hole transporting materials;
Organic HTMs;
Inorganic HTMs;
Carbonaceous HTMs;
Photovoltaic parameters

Abstract The rapid increase in the efficiency of perovskite solar cells (PSCs) in last few decades have made them very attractive to the photovoltaic (PV) community. However, the serious challenge is related to the stability under various conditions and toxicity issues. A huge number of articles have been published in PSCs in the recent years focusing these issues by employing different strategies in the synthesis of electron transport layer (ETL), active perovskite layer, hole transport layer (HTL) and back contact counter electrodes. This article tends to focus on the role and classification of different materials used as HTL in influencing long-term stability, in improving the photovoltaic parameters and thereby enhancing the device efficiency. Hole Transport Materials (HTMs) are categorized by dividing into three primary types, namely; organic, inorganic and carbonaceous HTMs. To analyze the role of HTM in detail, we further divide these primary type of HTMs into different subgroups. The organic-based HTMs are subdivided into three categories, namely; long polymer HTMs, small molecule HTMs and cross-linked polymers and the inorganic

* Corresponding authors.
E-mail addresses: sharewithselva@gmail.com (S. Pitchaiya), vishnukutty2002@yahoo.co.in (M. Natarajan).
Peer review under responsibility of King Saud University.

Production and hosting by Elsevier

https://doi.org/10.1016/j.arabjc.2018.06.006

Please cite this article in press as: Pitchaiya, S. et al., A review on the classification of organic/inorganic/carbonaceous hole transporting materials for perovskite solar cell application. Arabian Journal of Chemistry (2018), https://doi.org/10.1016/j.arabjc.2018.06.006

HTMs have been classified into nickel (Ni) derivatives and copper (Cu) derivatives based HTMs, p-type semiconductor based HTMs and transition metal based HTMs. We further analyze the dual role of carbonaceous materials as HTM and counter electrode in the perovskite devices. In addition, in this review, an overview of the preparation methods, and the influence of the thickness of the HTM layers on the performance and stability of the perovskite devices are also provided. We have carried out a detailed comparison about the various classification of HTMs based on their cost-effectiveness and considering their role on effective device performance. This review further discusses the critical challenges involved in the synthesis and device engineering of HTMs. This will provide the reader a better insight into the state of the art of perovskite solar devices.

Contents

1. Introduction

Methylammonium lead halide ($CH_3NH_3PbX_3$, X = Cl, Br or I) type perovskite solar cells (PSCs) have shown remarkable improvement in power conversion efficiencies (PCE) over the past decade. The inherent properties of the perovskite materials such as; ambipolar transport characteristics over a long range, high dielectric constant, low exciton binding energy, and intrinsic ferroelectric polarization have made this possible (Hsiao et al., 2015). The increase in PCE from 3.8% to 22.1% within the short span of time has been achieved through typical material synthesis and easy device engineering with solution processability, low-cost, and high-power conversion efficiency. Correspondingly, the hole-transport and electron-transport layers also play a key role in determining the resultant device performance, which is dependent on the charge extraction characteristics (Abdulrazzaq et al., 2013; Noh et al., 2013). To further increase PCE, most of the research is now focused on optimization of monolithic tandem silicon-based PSCs which have achieved efficiency above 25% (Correa-Baena et al., 2017).

In a typical cell architecture, an active perovskite absorber layer with a thickness of a few hundred nanometers is sandwiched between electron and hole transport layers (ETL and

Please cite this article in press as: Pitchaiya, S. et al., A review on the classification of organic/inorganic/carbonaceous hole transporting materials for perovskite solar cell application. Arabian Journal of Chemistry (2018), https://doi.org/10.1016/j.arabjc.2018.06.006

HTL). When the device is illuminated by the sun, excitons are created in the absorber layer then the excitons are extracted by the electron/hole transporting carrier layer and finally the charges are collected at the appropriate electrodes as depicted in Fig. 1. Research in fabricating superior quality active layers to achieve higher efficiency is still underway. Further, additional efforts on modifying and improving HTMs are also being carried out to improve the overall device performance and to achieve better stability from its hygroscopic nature (Hsiao et al., 2015). Also, it is important to consider the photovoltaic characteristics such as open circuit voltage (V_{OC}), short circuit current density (J_{SC}), fill factor (FF), incident photon conversion efficiency (IPCE) and the response range of solar cell for the better performance of the device in PV technology. Till now a large number of reports on various organic HTMs such as spiro-OMeTAD, PEDOT:PSS, PTAA and P3HT (Burschka et al., 2013; Heo et al., 2013; Chen et al., 2013; Green and Emery, 1993; Cai et al., 2013; Ball et al., 2013) are available which have been used to provide higher open circuit voltage and achieve higher efficiencies, yet the industrial development and market potential of PSCs is restricted due to their high cost and instability in water, heat and light (Christians et al., 2014). To overcome these drawbacks, alternate HTMs must be identified which are inexpensive and stable under all ambient conditions. This has led to the identification of effective inorganic hole transporters such as NiO, Cu_2O, CuO, CuI, $CuCrO_2$, $CuGaO_2$, MoO_x (as an interlayer), VO_x and WO_x which are inexpensive, abundant, non-toxic and energy non-intensive (Christians et al., 2014; Subbiah et al., 2014; Wang et al., 2014; Jeng et al., 2014; Zhu et al., 2014; Hu

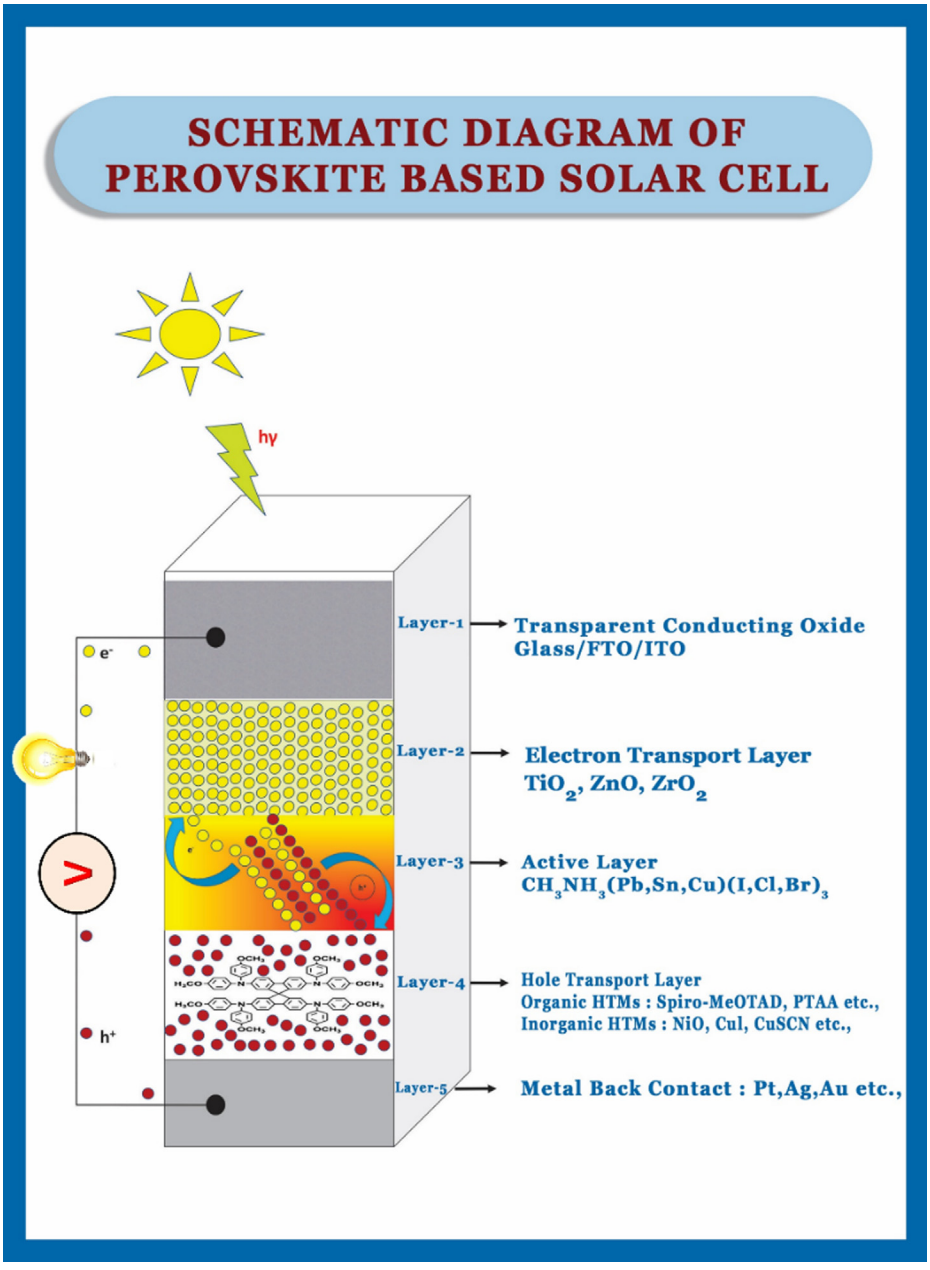

Fig. 1 Schematic representation of perovskite solar cell.

Table 1 List of recent reviews on various HTMs used in perovskite solar cells.

S. No.	Title of the paper	List of HTMs discussed	References
1.	Emerging of inorganic hole transporting materials for perovskite solar cells	**1. Nanoparticles as HTMs:** CZTS nanoparticles, WO_3 nanocrystals, NiO nanocrystals, CuS nanoparticles, $CuInS_2$ colloidal quantum dots, lead sulphide (PbS). **2. Inorganic HTM Based PSCs**: i. Copper-based HTMs: CuI, Cu_2O, CuO, and CuSCN. ii. Nickel-based materials as HTMs. iii. Carbon materials based HTMs: carbon, graphene QDs, and CNTs. iv. Miscellaneous inorganic HTMs such as Hybrid HTMs, GO and r-GO.	Rajeswari et al. (2017)
2.	Advances in hole transport materials engineering for stable and efficient perovskite solar cells	**1. Polymer-based HTMs:** **i. Small molecule-based HTMs:** Spiro-OMeTAD, dopants in spiro-OMeTAD and its derivatives. **ii. Alternative small molecule based HTMs:** Thiophene derivatives, Triptycene derivatives, Triazine derivatives, Porphyrin derivatives, Triphenylamine derivatives, Tetrathiafulvalene derivatives, Carbazole derivatives and Phthalocyanine derivatives. **iii. Long polymer based HTMs:** P3HT, PTAA, PEDOT: PSS. iv. Oligomer HTMs. **2. Inorganic HTMs:** CuI, CuSCN, NiO, Cu_2O, GO, MoO_3, VO_x, WO_3 nanocrystals and quantum dots.	Bakr et al. (2017)
3.	Hole transporting materials for mesoscopic perovskite solar cells –towards a rational design?	**1. Inorganic and organometallic HTMs:** CuI, Cu_2O, CuSCN. **2. Polymeric Organic HTMs:** PTAA, PPN, PIF8-TAA. **i. Small molecule organic HTMs:** triarylamine (TAA) and/or thiophene moieties. **ii. Spiro-OMeTAD and related molecules:** pm-spiro-OMeTAD and po-spiro-OMeTAD. **3. Organic HTMs:** Paracyclophane, Triptycene, and Bimesitylene. **4. Thiophene and Furan-based HTMs**. **5. Dendrimer-like and star-type HTMs**	Krishna and Grimsdale (2017)
4.	Recent progress of dopant-free organic hole-transporting materials in perovskite solar cells	**1. Dopant-free polymer HTMs:** Spiro-OMeTAD, PTB7, PCDTBT, PDPPDBTE, P3HT, and PTAA. **2. Dopant-free small molecule HTMs:** pBBTa-BDT1, pBBTa-BDT2 polymers, DERDTS-TBDT and DORDTS-DFBT.	Liu and Yongsheng (2017)
5.	Carbon-based perovskite solar cells without hole transport materials: the front runner to the market?	**1. Carbon based HTMs:** i. Meso C-PSCs ii. Embedment C-PSCs iii. Paintable C-PSCs	Chen et al. (2017)
6.	Hole-transport materials for perovskite solar cells	**1. Inorganic p-type semiconductors as HTMs:** CuI, CuSCN, NiO. **2. Organometallic HTMs:** Tetramethyl-substituted CuII phthalocyanine (CuMePc), green non-aggregated ZnII octa(2,6-diphenylphenoxy) phthalocyanine. **3. Conjugated polymers as HTMs:** PEDOT: PSS, P3HT, PTAA. **4. Small-organic HTMs:** Spiro-bifluorenes, Thiophenes, Triphenylamines, Triazatruxenes, Azulenes, Other Small Organic Molecules HTMs.	Calió et al. (2016)
7.	Hole-transporting materials for perovskite-sensitized solar cells	**1. Organic HTMs:** i. **Small-molecule p-type semiconductors:** Spiro-OMeTAD, DMeO-TPD, Tetrathiafulvalene (TTF), DR3TBDTT, N, N, N', N'-Tetraphenylbenzidine phenyl derivatives, Pyrene derivatives, DATPA diphenylamine group derivatives, Triazine-based HTMs, Triptycene-based HTMs. ii. **Polymer p-type semiconductors:** P3HT, PCBTDPP, PTAA, PDPPDBTE. iii. **Oligomeric organic HTMs.** **2. Inorganic HTMs:** NiO, CuSCN, PbS CQD (colloidal QDs)	Dhingra et al. (2016)
8.	Hole-transporting materials in inverted planar perovskite solar cells	**1. Conductive polymers:** PEDOT: PSS and its Derivatives. **2. Polythiophene and other polymers.** **3. Inorganic *p*-type semiconductors:** NiO_x, CuSCN, Cu_2O, and V_2O_5.	Yan et al. (2016)
9.	Perovskite solar cells: influence of hole transporting materials on power conversion efficiency	**1. Organic small molecules:** Py-A, Py-B, Triazine, OMeTPA-FA, MeO & Me_2N -DATPA. **2. Organic spiro-based molecules:** Spiro-OMeTAD, pm-spiro-OMeTAD, po-spiro-OMeTAD, KTM3. **3. Organic polymers:** PCBTDPP, PTAA, PDPPDBTE, PCPDTBT, PCDTBT, PFB, PANI. **4. Inorganic materials:** CuPC, CuI, CuSCN.	Ameen et al. (2016)

Please cite this article in press as: Pitchaiya, S. et al., A review on the classification of organic/inorganic/carbonaceous hole transporting materials for perovskite solar cell application. Arabian Journal of Chemistry (2018), https://doi.org/10.1016/j.arabjc.2018.06.006

Table 1 (*continued*)

S. No.	Title of the paper	List of HTMs discussed	References
10.	A review on the classification of organic/inorganic/carbonaceous hole transporting materials for perovskite solar cell applications	**1. Organic HTMs:** i. **Small molecule-based HTMs:** Pyrene, Thiophene, porphyrin, Carbazole. ii. **Long polymer based HTMs:** spiro-OMeTAD, fluorine doped spiro-OMeTAD and MoO_x (interlayer in spiro-OMeTAD), PEDOT: PSS, P3HT and PTAA. **2. Inorganic HTMs:** i. **Nickel & copper based HTMs:** NiO, CuI, Cu_2O, CuO, $CuCrO_2$, $CuGaO_2$. ii. ***p*-type semiconductors based HTMs:** CuPc, CuSCN. iii. **Transition metal-based HTMs:** MoO_3, V_2O_5, VO_x, WO_x. **3. Carbonaceous HTMs/electrode:** Conducting Carbon, CNTs, GO, r-GO.	Present review perspectives

et al., 2014; Tian et al., 2014; Ito et al., 2014; Qin et al., 2014). Since efficiency and stability are both essential in photovoltaics, these inorganic HTMs provide affordable stability but in terms of efficiency aspect it remains unsatisfied. whereas the important aspect is to achieve the both i.e. efficiency and stability using one HTM. Thus, carbon has been identified as a potential HTM in terms of efficiency and long-term stability. Its approximate work function of ~5.0 eV makes it an ideal material to replace other costly and unstable HTMs in PSCs. Considering the above facts various HTMs have been introduced recently in PSCs which have been displayed in Table 1. Herewith, some of the recent reviews have been analyzed and discussed. Among these, Rajeswari et al. (2017) have reported about the efficiency and stability of PSCs fabricated using various metal oxide HTMs. They have given an overview of both organic and inorganic HTMs and concluded that inorganic HTMs are better market competitors than organic HTMs. Bakr et al. (2017), carried out a review on PSCs with polymer-based HTMs used in PSCs. They have provided a critical analysis on the role of structure, electrochemistry and physical properties of HTMs made of small molecules, long-chain polymers, organometallic and inorganic materials and their effect on photovoltaic parameters of PSCs fabricated in various device configurations. Krishna and Grimsdale (2017), have provided an overview of the various types of newly proposed polymeric HTMs, organic and organometallic based HTMs. They have highlighted the enabling rational design of a cost-effective PSC device fabricated using polymeric based HTMs which is better in terms of performance when compared to the PSC devices constructed using organic HTMs. Liu and Yongsheng (2017), have reviewed the latest developments of conventional PSCs with a focus on dopant-free organic HTMs, and they have stated that the energy-level tuning of the HTMs plays a key role in obtaining efficient dopant-free HTL for PSC technology. Recent progress on carbon-based PSCs, including meso-PSCs, embedment PSCs and paintable PSCs, has been reviewed by Chen et al. (2017). They have reported that the device structure and working principle of carbon-based PSCs are different from other HTMs and tends to provide an efficient cost-effective PSCs to the photovoltaic (PV) community (Wang et al., 2016). Calió et al. (2016) provided a brief review on the organic and inorganic p-type semiconductors, giving an assessment on the modification and optimization of various p-type HTMs for the stable and efficient PSCs. With an aim to find an alternative for the expensive spiro-OMeTAD based HTMs (Dhingra et al., 2016) discussed about the performance of organic (further divided into three classes; small-molecule, oligomeric HTMs, polymeric HTMs) and inorganic HTMs. The influence of mobility, work function and film property on the performance of conductive polymer based HTMs of PSCs has been discussed by Yan et al. (2016). Ameen et al. (2016) have studied about the role of interaction between the perovskites and HTM of PSCs with respect to stability and efficiency. An overview of the recent reviews based on various HTMs used in PSCs has been given in Table 1.

In this review article, we have discussed about the classification of the organic/inorganic materials used so far in PSCs coming under the three major categories namely; organic

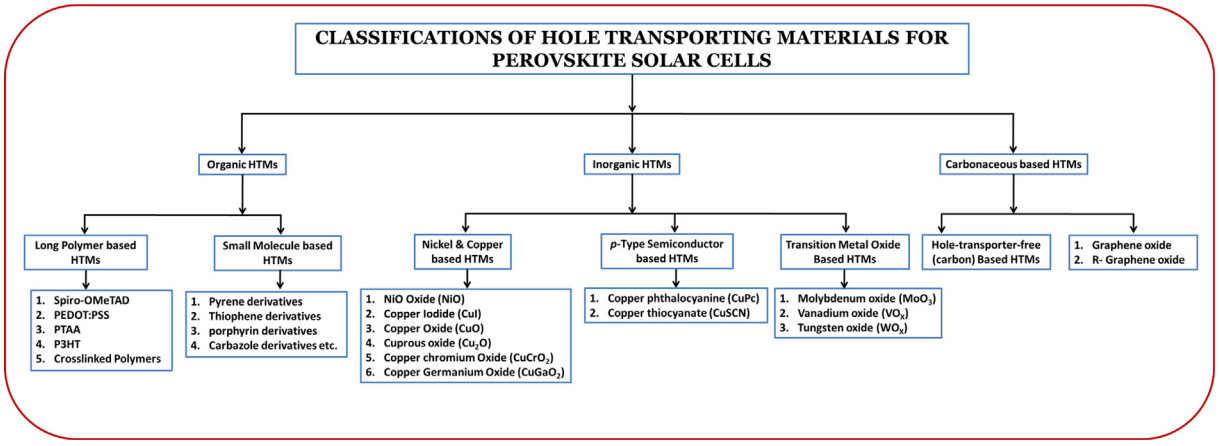

Fig. 2 Flow-chart illustrating the classification of hole transporting materials (HTMs) discussed in the present article.

HTMs, inorganic HTMs and carbonaceous based HTMs/electrodes. Further, the organic-based HTMs are subdivided into long chain polymer HTMs and small molecule HTMs. The inorganic HTMs have been divided into nickel-based HTMs, copper-based HTMs, p-type semiconductor based HTMs and transition metal based HTMs. Fig. 2, shows the flow chart about the classification of the HTMs discussed in the present review. This proposed review also tends to provide an overview on the significant progress of various HTMs used in PSCs to give an overall knowledge on the selection and introduction of new hole transport materials which can make perovskite-based solar cells a market viable.

2. Evolution on perovskite device architecture

An understanding of evolution in PSC device architecture will be helpful in adopting suitable HTMs to enhance the performance and long-term stability, which will be a significant criterion for the commercialization. There is no doubt that recent research in introducing various interfacial transporting layers will help to improve and solve the above-said issues which are currently observed in PSCs.

Herein, we have provided a brief introduction on the evolution of perovskite device architecture and its influence on the selection of HTMs. Factually, PSCs emerged at first as a sensitized solar cell replacing DSSCs in terms of liquid dye/electrolyte by perovskite absorber material which is having 15–20 times higher absorption coefficient (Kojima et al., 2009). Perovskite solar cells seem to provide a wide variety of device architecture than all the other community in PV technology. Herein, Fakharuddin et al. (2016) have classified this wide variety of design in PSC device based on its conductivity nature (n or p-type), morphology (mesoporous and meso-superstructure) and structure (n-i-p or p-i-n and p-n or n-p devices) as shown in Fig. 3(a)–(f).

Based on the electrical properties (whether electrons or holes are collected at the bottom transparent conducting oxide (TCO)) of the device, Mali and Hong (2016) classified the perovskite structure into two major categories; (1) normal/regular p-n type and (2) planar either n-i-p (conventional planar) or p-i-n (inverted planar) type. This, conventional planar structured perovskite device can be further divided into two namely; (i) mesoporous and (ii) meso-superstructure as shown in Fig. 4 (a)–(d). Batmunkh et al. (2015) have provided an overview on the evolution of the PSC architecture and its progress in terms of efficiency (3.8% by Miyasaka's group (2009) to 18% by Yang's group (2014)) and which depends on the device architecture. Similarly, Momblona et al., have fabricated p-i-n and n-i-p PSCs by employing doped charge transport layers in the device design and achieved a higher PCE of 20.3 (2017)% (Momblona et al., 2016). HTM-free based PSCs displays an improved performance from 5.5% to 12.8% in both planar and mesoscopic heterojunction arrangement. Further, these advancements were achieved by using conducting interfacial engineering, thickness optimization of transporting and perovskite layers and by, introducing new scaffold layers (Teh et al., 2016).

2.1. Role of HTMs in PSC device structure

The stability and performance depends on the transporting layers used in the device architecture as it serves the various aspects in PSCs such as; (i) it acts as a physical/energetic barrier between ETL and perovskite layer by blocking the electron transfer; (ii) by improving the hole transporting efficiency due to its high hole mobility and its matching energy level with those of ETMs/HTMs and electrode, (iii) avoids the degradation and corrosion which can take place in the absence of an HTM at the metal-perovskite interface (Salim et al., 2015). (iv) suppresses charge recombination by fully separating the

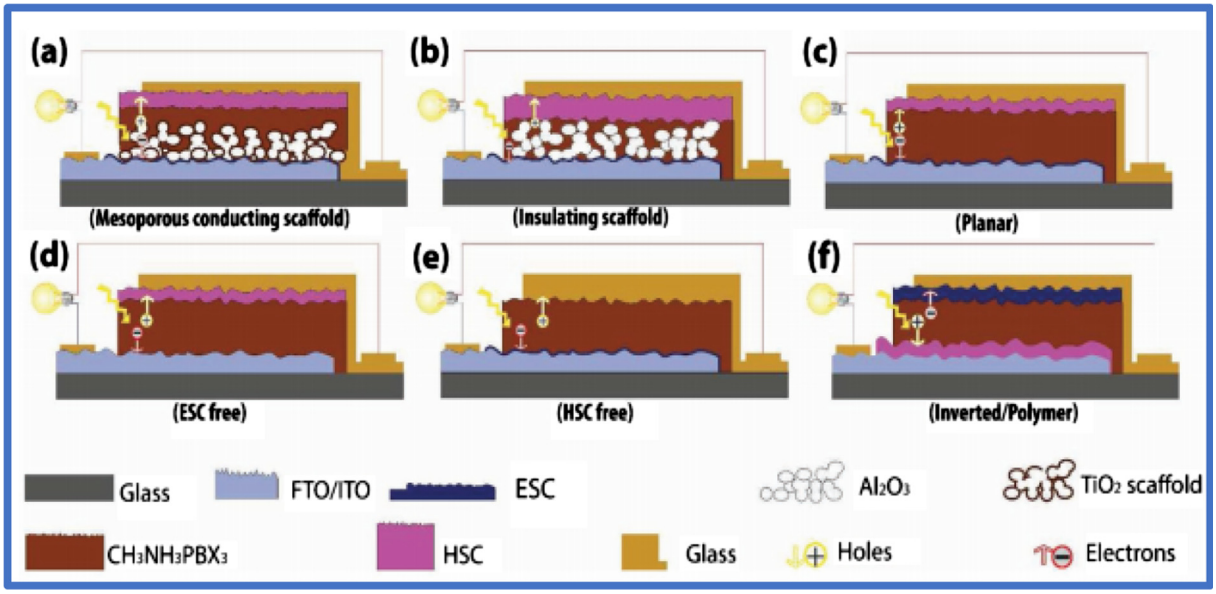

Fig. 3 Schematic on the various perovskite device architecture (a) mesoporous (b) meso-superstructure (c) planar (d and e) ETM/HTM free (f) polymer structured PSCs. Figure adapted with permission from Ref. (Fakharuddin et al., 2017) Copyright of AIP Publishing.

Please cite this article in press as: Pitchaiya, S. et al., A review on the classification of organic/inorganic/carbonaceous hole transporting materials for perovskite solar cell application. Arabian Journal of Chemistry (2018), https://doi.org/10.1016/j.arabjc.2018.06.006

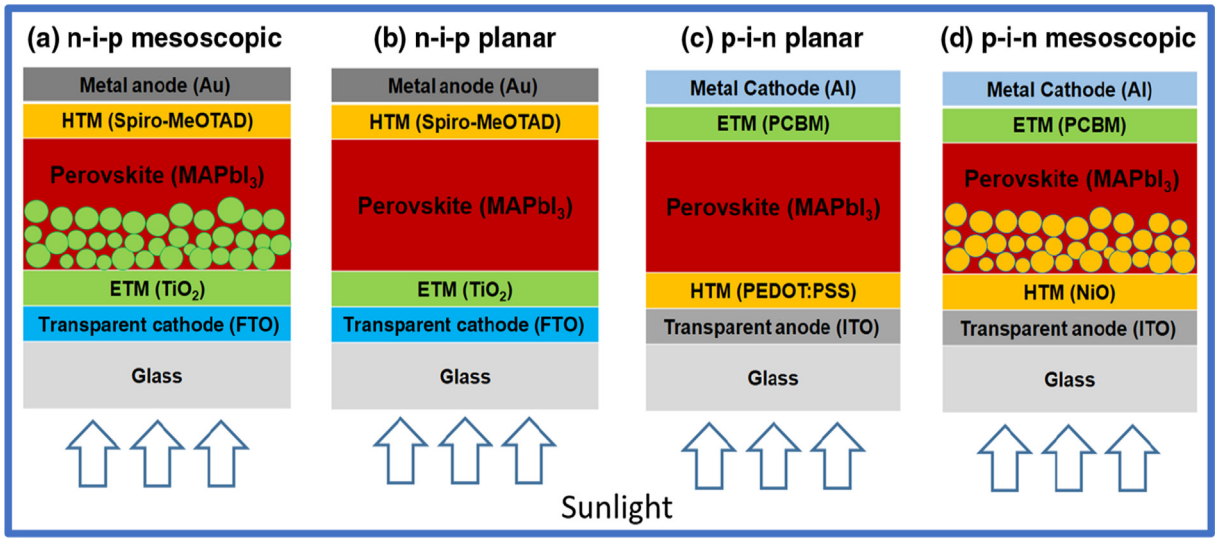

Fig. 4 (a-d) Schematic showing classification in (n-i-p and p-i-n) planar and mesoscopic structured perovskite device. Figure adapted with permission from Ref. (Song et al., 2016).

top contact from the bottom transport or contact layer leading to improved performance. Though we have a wide variety of device architectures available for achieving both stability and performance, besides this HTMs play the most vital in swapping environmental and economic drawbacks of the perovskite solar cells which are under scrutiny. The light-to-electricity conversion in PSCs can be further improved by using suitable HTMs with well-established device architecture.

2.2. Remarkable properties of HTM in PSCs

HTMs play an important role in determining the device performance and the researchers must consider the following aspects for the introduction of new HTMs; It should have suitable energy levels, providing the driving force for charge transfer (i.e. the highest occupied molecular orbital, HOMO, energy levels of the selected HTMs must be slightly higher to that of the perovskite materials). It should act as a barrier between anode and perovskite layer to block electrons without entering the anode (i.e. its lowest unoccupied molecular orbital, LUMO, energy level should be significantly lower than that of the perovskite absorber). It should have a high hole transfer efficiency (possibly $> 10^{-3}$ cm^2 V^{-1} s^{-1}) to facilitate hole conduction and prevent charge recombination. It should favor the open circuit voltage by determining the splitting of the quasi fermi-energy levels of the perovskite (Bakr et al., 2017). It should also avoid the diffusion between back electrode metal and the perovskite layer. It should be cost-effective and should have high thermal stability and resistance to external degradation factors such as moisture and oxygen for a long-term device performance and must be environment friendly.

2.3. Stability perspectives of HTMs in PSCs

The high yielding perovskite devices suffer from extreme instability towards air, water, moisture, light and heat which may be due to the instability in both the perovskite and the transporting layers. The researchers have demonstrated that replacing the lead based perovskite material with any other component may not be suitable in achieving higher performance. So, the focus is on choosing suitable HTMs. The potential to use organic material as HTMs for solar cell technology was first observed in 1975 (Tang, 1986), but that resulted in very low efficiency. After enormous effort, an efficiency of 3.8% was achieved. In 1998, Bach et al. (1998), reported about HTMs based on spiro-OMeTAD, which displayed an open-circuit voltage exceeding 0.9 V but yielded only 2.56% PCE. Then the same group in 2012, achieved an efficiency of about 9.1% after various optimizations made in transporting layers paved way to introduce long-chain polymer based HTMs such as spiro-OMeTAD, PEDOT: PSS, PTAA, and P3HT. But the problems related to instability in using these organic long chain polymers based HTMs remains a challenge. Also, this spiro-OMeTAD as HTM, requires costly additive (4-tert-butylpyridine) and dopants (typically hygroscopic Li-salts) as it suffers from poor instability caused by the spiro structure. To overcome such drawbacks the spiro-skeleton could be replaced with other ensemble to improve the stability of the interface between perovskite/HTL. Li et al. (2014), incorporated montmorillonite (MMT) as a buffer layer between spiro-OMeTAD and perovskite to improve the stability towards ambient conditions. To further improve the stability, one of the most striking approach was incorporation of spiro $(TFSI)_2$ as HTM to replace pristine spiro-OMeTAD. Researchers have also focused on PEDOT: PSS, its acidic nature is a concern for the long-term stability of solar cells. It also produces a lower PCE due to low hole mobility, it is sensitive to humidity and is expensive (Nguyen et al., 2014). Also, the cost of these organic materials, the dopants and the additives are very high. These drawbacks have forced researchers to find low cost materials with long-term stability. This has brought inorganic p-type materials such as copper, nickel, transition metal oxide based HTMs (CuI, NiO, Cu_2O, CuO, MoO_x, VO_x, WO_x) into PSCs. These inorganic materials have wider band gap, high conductivity and also prevents the device from exposure to the ambient atmosphere. So employing such inorganic materials in PSCs could help to achieve higher PCE, yet their sensitivity towards oxygen and moisture seems to be a

Please cite this article in press as: Pitchaiya, S. et al., A review on the classification of organic/inorganic/carbonaceous hole transporting materials for perovskite solar cell application. Arabian Journal of Chemistry (2018), https://doi.org/10.1016/j.arabjc.2018.06.006

hindrance. To address these issues of sensitivity towards ambient condition, carbon based materials have been used photovoltaics as an electrode in PSC. With its low-cost and abundant availability on earth, it becomes an ideal candidate for hole-conductor. Though carbon emerged as an electrode, its favorable photovoltaic properties makes it to play dual role in PSCs (both as an electrode and as a HTM) which has invoked researchers to focus on carbon and its derivatives based materials which can be used as replacement to other high cost, unstable and sensitive HTMs. Hence, in this review article, a complete detail about the different available organic/inorganic/carbonaceous based HTMs is provided.

3. HTMs versus J-V hysteresis behavior

The role of HTMs in PSCs and the effect of the choice of hole transport material on the J-V hysteresis behavior is being discussed and it is an essential factor in determining the efficiency of PSCs. According to Chen et al. (2016) the photocurrent density-voltage (J-V) behavior of the PSCs exhibit strange dependence on the voltage scan direction, scan rate and scan range, giving rise to hysteresis behaviour. Such J-V hysteresis effect causes serious cell stability problems and difficulties in determining the cell efficiency. This anomalous J-V hysteresis behavior has been observed for various PSC configurations such as planar PSCs, mesoporous PSCs, HTL-free PSCs, and inverted polymeric perovskite devices. This anomalous J-V hysteresis behavior of PSC devices fabricated using various HTM materials has been shown in Fig. 5(a)–(d). Kim et al. (2015), observed J-V hysteresis for the mixed halide perovskite $CH_3NH_3PbI_{3-x}Cl_x$ and the J-V hysteresis was found to be significantly dependent on the p-type HTM materials used. Here they have systematically examined the impact of interface-dependent electrode polarization on the J-V hysteresis for different HTMs. They have demonstrated that the hysteresis became negligible when the capacitance was much reduced and found that the replacement of Spiro-OMeTAD with PEDOT: PSS or any other inorganic HTM can further decrease the capacitance to a value of 10^{-5} F/cm^2, leading to a hysteresis-free behavior (given in Fig. 5a and b). Therefore, HTM layers in the normal perovskite based solar cell structure plays critical role in the electrode polarization and affects the J-V hysteresis. The PV performance of P3HT based PSCs is generally lower than spiro-OMeTAD - based PSCs due to the low hole mobility of the former (shown in Fig. 5c). Furthermore, through trapping and de-trapping processes one can explain the difference in PV performance between the reverse and forward scans due to different extraction efficiencies of holes by the HTMs used. With this, we can also mention that the evolution of J-V hysteresis is also due to the trapping and de-trapping process. Further, Habisreutinger et al. (2014), Abdulrazzaq et al. (2013) examined the effect of Li-TFSI and tBP additives on the device performance having a PCE ~ 13.7%, for doped P3HT, higher than a pristine (PCE ~ 5.7%). Recently Yin et al. (2017) reported, almost no hysteresis for NiO_x and for the PCBM based device in Fig. 5d. As a result, PCE of 15.71% was obtained. Hence, the passivation of charge traps in perovskite thin films can

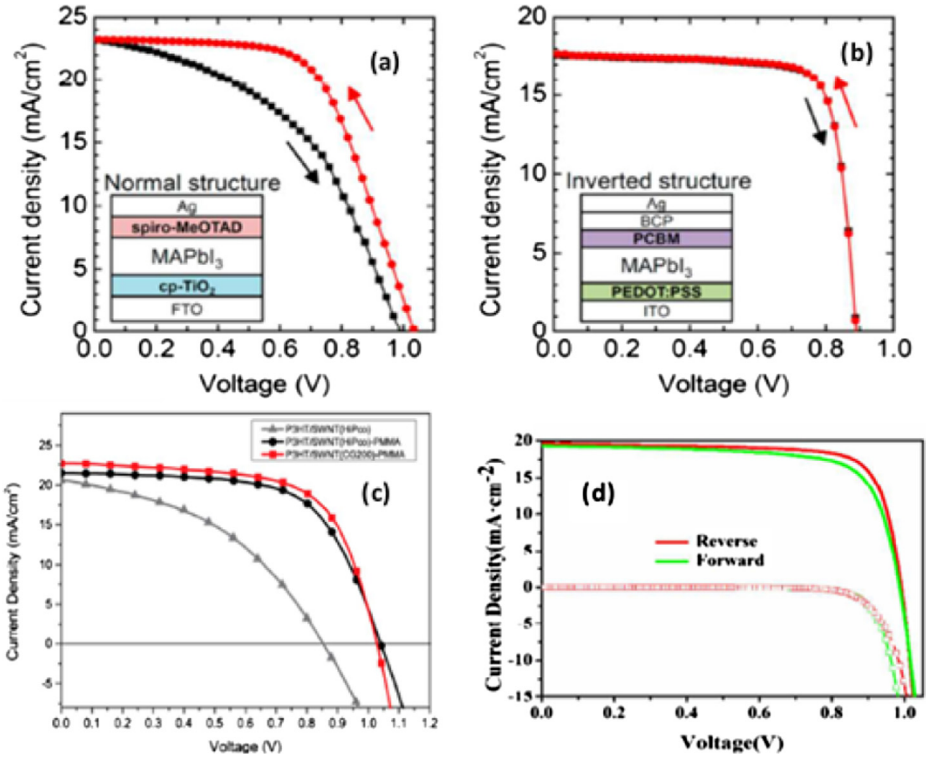

Fig. 5 The J-V behavior of forward and reverse scan directions for different HTM (a) Spiro-OMeTAD (b) PEDOT: PSS, (a – b) reproduced with permission from Ref. (Chen et al., 2016). Copyright 2016 ACS. (c) P3HT as HTM, the figure is reproduced with permission from Ref. (Habisreutinger et al., 2014). (d) NiO as HTM, the figure is reproduced with permission from Ref. (Yin et al., 2017).

eliminate the hysteresis, which indicates that the influence of charge traps on hole extraction efficiency can be improved by using different dopants in HTMs. Similarly, Wei et al. (2015) have investigated the photocurrent hysteresis effect in the as-fabricated carbon-based PSCs (shown in Fig. 6). They have obtained J-V curves with different scan direction and discussed about the importance of hysteresis and how it affects both stability and performance of the PSC devices. After preliminary optimization of the hysteresis behavior of the carbon-based HTMs, they could achieve a hysteresis-free J-V characteristics with PCE of 12.67% with a very impressive FF of 80%. This hysteresis analysis opens new opportunities for designing and assembling nanostructured and highly conductive carbon cathode as HTM in PSCs. From this it is understand that the role of HTM is very important and can provide important insight not only in unraveling but also in attenuating the J-V hysteresis which in turn plays a role in determining the PCE of the PSCs.

4. Classification of organic hole transporting materials

Organic polymers, in general, consist of chains of repeating units and the complexities are in between small molecules and long-chain monomers with the distribution of carbon molecules. In most cases, the structures of small molecules and chained polymers are obtained in such a way that they possess suitable photovoltaic properties such as charge mobility, luminescent property, or light absorption property for PV device applications (Lattante, 2014).

4.1. Classification of organic long chain polymer HTMs

(Prisitne & Doped spiro-OMeTAD/PEDOT: PSS/P3HT/PTAA & Cross-linked polymers)

In this topic, we will be focusing on the latest development of the different organic conducting polymers (both long chain and small molecules), small molecules and crosslinked polymers based hole transporting material to analyze the transport properties of polymeric PV materials and have correlated and compared the results on device performance and stability.

4.1.1. ***Spiro-OMeTAD based HTMs:*** *(Prisitne spiro/fluorine doped spiro-OMeTAD HTMs)*

Spiro-OMeTAD (2,2′,7,7′-Tetrakis-(N,N-di-4-methoxypheny lamino)-9,9-spirobifluorene) is one of the most commonly used HTM in PSCs because of its several desirable properties like favourable glass transition temperature (Tg = 120 °C), solubility, ionization potential, absorption spectrum and solid-state morphology (Huang et al., 2016). It has also been found to be the most suitable HTM for the fabrication of PSCs due to its facile nature and high device performance (Hawash et al., 2018).

Bach et al. (1998) were the first to introduce spiro-OMeTAD in DSSCs and they used it as an efficient heterojunction layer

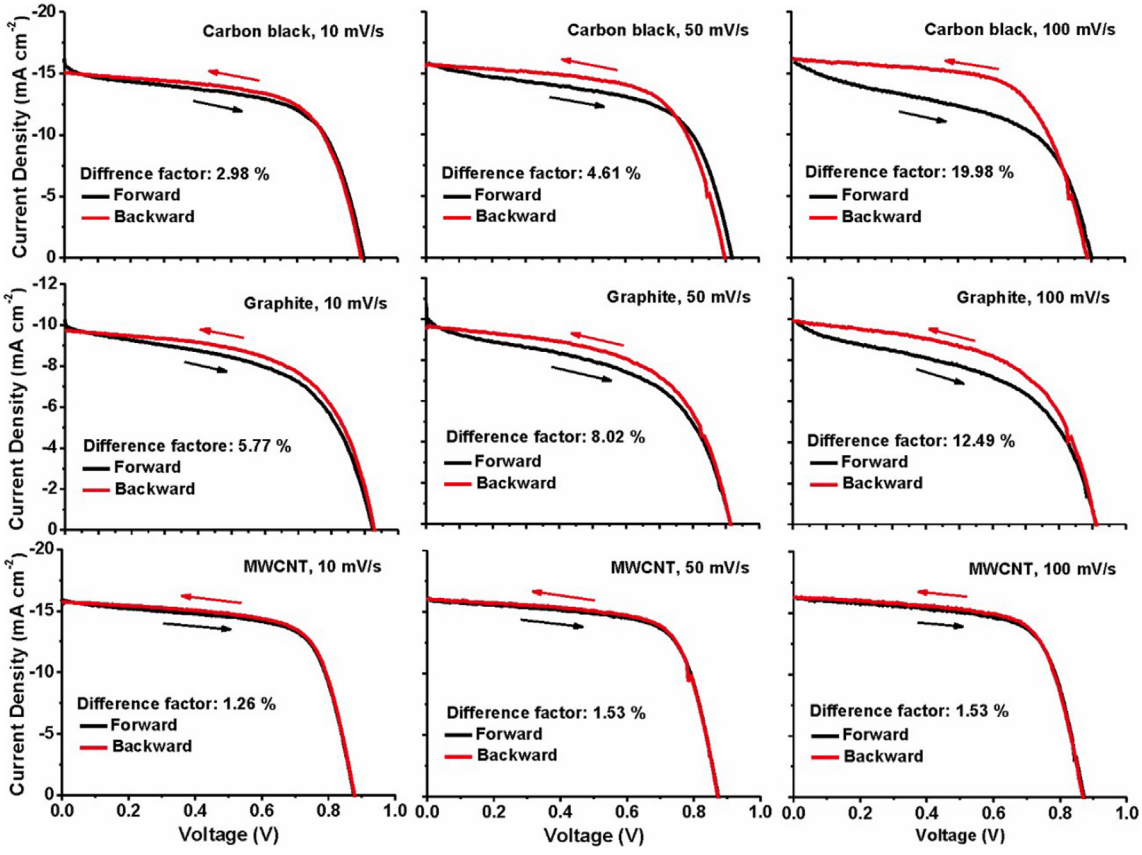

Fig. 6 Hysteresis effect in the as-fabricated carbon-based HTMs such as carbon black, graphite and MWCNT. This figure is reproduced with permission from Ref. (Wei et al., 2015).

formed with dye absorbers resulting good PCE. Following this, many researchers widely adopted spiro-OMeTAD as HTM in solid state DSSCs. After this, perovskite solar cells emerged and created a leading breakthrough in PCEs exceeding 22% by using spiro-OMeTAD (Hawash et al., 2018). Though their results reveal the improved performance but yet the devices suffer from the instability towards water, light, and heat due to the instability of spiro-OMeTAD that mainly originates from its amorphous nature and its chemical structure. To overcome this prisitine and various doped spiro have been used as HTM in PSCs. The first additive employed in spiro-OMeTAD were lithium and antimony-based salts Li[$(CF_3SO_2)_2N$] (Li-TFSI) by Burschka et al. (2013) and they have achieved the highest PCE at that time in solid state DSSCs with a PCE of 7.2%. The role of this antimony salt as dopant is to produce free charge carriers in the HTM via the oxidation of spiro-OMeTAD. Then the ionic lithium salt additive dopants provide the Li^+ ions to the system. Though spiro-OMeTAD based HTMs doped with Li-TFSI to improve the performance, the extreme hygroscopic nature of lithium salt seriously accelerates the decomposition of perovskite and degrades the device performance. The presence of pinhole channels originating from the migration of Li-TFSI from the bottom to the top across the spiro-OMeTAD film can promote the degradation processes (Hawash et al., 2015). Wang et al. (2016) have shown that tBP plays a major role in homogenizing the HTM and have also shown that tBP works as a morphology controller and prevents Li-TFSI accumulation and segregation even in the stock solution. The addition of acetonitrile in Li-TFSI improves the electronic properties of PSCs, but the addition of tBP corrodes the perovskite layer which in turn leads to instability (Krishnamoorthy et al., 2014).

In PSCs, various dopants have been used in the spiro-OMeTAD based HTMs so as to enhance its electrical conductivity, stability. Based on these considerations, Hua et al. (2016) have used fluorine-doped spiro-OMeTAD and tried to enhance the stability of PSCs. Doping non-hygroscopic materials such as tetrafluoro-tetra cyanoquinodimethane [F4-TCNQ] in spiro-OMeTAD helps in improving the device efficiency. So they have systematically investigated the influence of the structural molecular modification of the HTMs (2,7-dibromo-9H-fluorene and 4,4,′-dimethoxydiphenylamine-HT1) and 4-Bromo-N,N-bis(4-methoxyphenyl)aniline, catalyzed by Pd(dba)2-HT2) on PSCs performance. Their results indicate that the extended three-dimensional structure and higher molecular weight of HT2 enables better photovoltaic performance but do not help in improving stability. Recently, Hawash et al. (2018) have reported that spiro-OMeTAD with various new additives and dopants used nowadays outperforms the performance of prisitine spiro-OMeTAD both in terms of performance and stability. Further, Ou et al. (2017) have stated that the energy offset between the perovskite and the spiro-OMeTAD has to be small enough in order to achieve a high V_{OC}.

Li et al. (2017) have examined the effectiveness of adding a variety of moderate-to-strong acids (H_3PO_4, CF_3PA, H_2SO_4, AcOH) to spiro-OMeTAD formulation in $FA_{0.85}Cs_{0.15}PbI_3$-based PSCs. From their J–V curves, it was a quite evident that all cells using acid-based HTL exhibit improved device performance and the improvement mainly results from increased V_{OC} and FF. Interestingly, the improvement is almost identical regardless what acid was used as the additive to the HTL formulation. It is important to highlight that the acidity of these acids covers a wide range from –3 (H_2SO_4) to 4.75 (AcOH), and these acids also have very different counter anions (HSO_4^-, $H_2PO_4^-$, CF_3PA^-, AcO^-). Thus, the performance improvement with acid addition in HTL was independent of the specific acidity and type of acids and strongly suggests that the acid additive is a general strategy for improving charge conduction in HTMs and consequently enhancing the performance of PSCs. The consistent and significant improvement of V_{OC} obtained using acid-based HTM also suggests that the acid additive could affect the interface between HTM and perovskite and helps to reduce the overall recombination losses. The acid additives effectively improves the conductivity of spiro- OMeTAD doped by Li-TFSI and/or Co (III) salts. Thus, in their aspect of research using acid additives may be a promising general approach to enhance conductivity of spiro-OMeTAD and hence develop high-efficiency hysteresis-less PSCs.

Highly conductive Ni nanobelts can be viewed as an efficient hole collector which can reduce the hole transfer path and accelerate its transfer rate from perovskite to back electrode (Liu et al., 2017). They have optimized and found that 1.8 mg/mL of Ni nanobelts based devices with the advantages of enhanced hole extraction and transport resulted in up to ~ 22% PCE when compared to the pristine device (15.57% – 12.76%). Despite the small J-V hysteresis, a higher PCE as high as 14.47% could be achieved for the devices fabricated with 1.8 mg/mL Ni nanobelts compared to the pristine spiro based HTM (12.05%). Ni nanobelt based PSCs also displayed outstanding ambient stability under a controlled humidity condition of ~30–40% in the dark. Overall, their work provides a new insight into the design and fabrication of effective HTM, which would undoubtedly facilitate the production of PSCs with high efficiency as well as long-term stability.

Li et al. (2016) have demonstrated that solution-processed composite film made of copper salt (CuSCN or CuI) doped spiro-OMeTAD behaves as a stable hole transport layer in perovskite solar cells. The doping which introduces p-type conductivity results in improved film conductivity and hole mobility in spiro-OMeTAD:CuSCN (or CuI) composite films, which is beneficial for hole transport and extraction. Accordingly, the PCE is improved from 14.82% to 18.02% owing to the obvious enhancements in the cell parameters. In addition, the introduction of inorganic copper salts can suppress the film aggregation and crystallization of spiro-OMeTAD films with reduction in pinholes and voids, which slows down the perovskite decomposition due to the prevention of moisture infiltration to some extent.

Also, several other dopants have been employed in spiro-OMeTAD based HTMs, such as Ag-TFSI, WO_3, CuI, $SnCl_4$, and Keggin-type polyoxometalates with all the works reporting some enhancement in both performance and stability. Though introduction of new materials as a dopant/additives in spiro-OMeTAD improves the device performance the stability remains a big challenge.

The device structure, method used for the preparation of HTM, thickness of the HTMs used, the IPCE and photovoltaic parameters of the PSCs fabricated using spiro-OMeTAD and doped spiro-OMeTAD as HTMs has been given in Table 2.

Please cite this article in press as: Pitchaiya, S. et al., A review on the classification of organic/inorganic/carbonaceous hole transporting materials for perovskite solar cell application. Arabian Journal of Chemistry (2018), https://doi.org/10.1016/j.arabjc.2018.06.006

Table 2 Photovoltaic characteristics of PSCs using spiro-OMeTAD and various doped spiro-OMeTAD based HTMs.

S. No.	Device gestalt	Structure type	Spiro-OMeTAD (HTM)		IPCE (response range) (nm)	Photovoltaic parameters				Ref.
			Method	Dopant material		V_{OC} (V)	J_{SC} (mA/cm^2)	FF (%)	η (%)	
1.	FTO/TiO_2/PSK/Pristine- spiro-OMeTAD/Ag	Planar p-i-n	Spin coating	Pristine spiro-OMeTAD	300–800	1.12	22.90	73	18.7	Habisreutinger et al. (2017)
2.	FTO/SnO_2/$FA_{0.83}MA_{0.17}Pb$ $(I_{0.83}Br_{0.17})_3$/ SWNTs- spiro-OMeTAD/Ag	Planar p-i-n	Spin coating	Single walled carbon nanotubes (without Li- TFSI + tBP)		1.14	22.10	75	18.9	
3.	FTO/TiO_2/PSK/Li-TFSI + tBP + spiro/Ag	Planar n-i-p	Spin coating	Li- TFSI + tBP		0.97	19.70	64	12.66	Di Giacomo et al. (2014)
4.	FTO/TiO_2/PSK/HT1 & HT2 + spiro-OMeTAD/Al	Planar n-i-p	Spin coating	Fluorine doped spiro		1.11	21.40	73	18.04	Hua et al. (2016)
7.	FTO/TiO_2/PSK/F4-TCNQ + spiro-OMeTAD/Ag	Planar n-i-p	Spin coating	Tetrafluoro-tetra cyano quino dimethane		0.94	18.72	48	10.59	Huang et al. (2016)
8.	FTO/TiO_2/$FA_{0.85}Cs_{0.15}PbI_3$/spiro with H_3PO_4 acid/Ag.	Planar p-i-n	Spin coating	H_3PO_4 acid		1.06	21.90	76	17.6	Li et al. (2017)
9.	FTO/TiO_2/$FA_{0.85}Cs_{0.15}PbI_3$/spiro + CF_3PA/Ag	Planar p-i-n	Spin coating	CF_3PA acid		1.04	21.60	78	17.5	
10.	FTO/TiO_2/$FA_{0.85}Cs_{0.15}PbI_3$/spiro with H_2SO_4 acid/Ag.	Planar p-i-n	Spin coating	H_2SO_4 acid		1.06	21.60	78	17.7	
11.	FTO/TiO_2/PSK/Ni-nanobelts + spiro/Ag	Planar p-i-n	Spin coating	Nickel nanobelts	350–750	1.02	21.64	73.3	16.18	Liu et al. (2017)
12.	ITO/TiO_2/PSK/CuSCN: spiro-OMeTAD/Ag	Planar p-i-n	Spin coating	Copper salts (CuSCN)	700–850	1.06	22.01	77	18.02	Li et al. (2016)
13.	ITO/TiO_2/PSK/CuI: spiro-OMeTAD/Ag	Planar p-i-n	Spin coating	Copper salts (CuI)	700–850	1.06	21.52	73	16.67	

Please cite this article in press as: Pitchaiya, S. et al., A review on the classification of organic/inorganic/carbonaceous hole transporting materials for perovskite solar cell application. Arabian Journal of Chemistry (2018), https://doi.org/10.1016/j.arabjc.2018.06.006

4.1.2. PEDOT: PSS polymer based HTMs

Jiang et al. (2017) have successfully applied a facile in-situ solid-state synthesis method to obtain a conducting poly (3,4-ethylene dioxythiophene) polystyrene sulfonate polymer (PEDOT: PSS) HTM, directly on top of perovskite layer, in conventional mesoscopic PSCs. The PEDOT film possesses the HOMO energy level at –5.5 eV, which facilitates an effective hole extraction from the perovskite absorber and shows an excellent PCE of 17.0%. Thus, their finding highlights the potential application of PEDOT as a HTM for cost-effective and efficient PSC. One of the drawbacks of PSCs is their limited stability in non-inert atmosphere which can be rectified by the inclusion of PEDOT: PSS as HTL in the inverted device configuration. You et al. (2014) have adopted a low-temperature processing technique to fabricate high efficiency devices, where PEDOT:PSS and PCBM are used as hole and electron transport layers. For the device structure, PCE of 11.5% was obtained on rigid substrates (glass/ITO), and a 9.2% PCE was achieved for a polyethylene terephthalate/ITO flexible substrate. Luo et al. (2017) achieved higher PCE of 15.34% for GO modified PEDOT: PSS when compared to that of PEDOT: PSS (11.90%). This graphene oxide (GO) modified PEDOT: PSS was able to maintain 83.5% of the initial PCE value after aging for 39 days, indicating that the use of the GO-modified PEDOT: PSS instead of the unmodified PEDOT as HTL seems to be a good strategy for efficiently improving the performance and stability of PSCs. Usage of ethanol in the GO solution can partially remove the hydrophilic PSS material from the surface during the spin-coating of the GO solution, which can further improve the moisture resistance and decrease the contact barrier at the PEDOT: PSS surface. The superior wettability of the GO-modified PEDOT: PSS surface helps to form a high-quality perovskite layer with better crystallinity and fewer pinholes. Furthermore, this GO selectivity in the hole extraction can inhibit the recombination of holes and electrons at the interface between the perovskite/PEDOT: PSS.

4.1.3. P3HT polymer based HTMs

Poly (3-hexylthiophene) (P3HT) is a promising p-type polymer having high charge transfer and good environmental stability used in electronic devices which can be a suitable material for HTL in PSCs. However, the mismatch of band alignment with perovskite layer suppresses efficient charge extraction and transfer and this may result in significant loss of open-circuit voltage and also device performance deterioration. Di Giacomo et al. (2014), the first to report highest PCE of 9.3% just by tuning the energy level of P3HT and optimizing the device fabrication have demonstrated that their result on using P3HT as HTM material can be a suitable low-cost HTL for efficient PSCs. Nia et al. (2017) have reported about PSCs using P3HT as HTL and has discussed about the relationship between P3HT molecular weight (MW) and the photovoltaic characteristics of the solar cell. Their results clearly showed a strong dependence of the cell efficiency on the P3HT MW: the larger the MW, the higher the efficiency. The efficiency enhancement was mainly related to the increase of J_{SC} and FF as P3HT MW increases. The reason for this dependence can be attributed to two concomitant effects: an increase of the electron lifetime and the increased absorbance of P3HT, when its MW is increased. Zhang et al. (2016) have successfully introduced F4TCNQ doped P3HT as an efficient HTM in mesoscopic PSCs. The overall performance was significantly enhanced after the introduction of F4TCNQ into P3HT. Under optimal doping conditions (1.0%, w/w), an impressive PCE of 14.4% was achieved, which was considerably higher than that of pristine P3HT based devices (10.3%). The dramatic improvement of the PCE should be largely attributed to the increases of the photocurrent density and fill factor. After doping with 1.0% F4TCNQ, the conductivity of P3HT film was increased by more than 50 times. Furthermore, this P3HT:F4TCNQ composite HTM based PSCs also exhibited excellent long-term stability under ambient atmosphere with a humidity of 40%. More intriguingly, both the efficiency and long-term stability of PSC device containing F4TCNQ outperformed the most commonly used additive Li-TFSI for P3HT. Hence, F4TCNQ was demonstrated to be an effective p-dopant for P3HT-based HTMs in PSCs combining high overall performance and good long-term durability. Novel large π-conjugated carbon material graphdiyne (GD) as a dopant in P3HT HTM layer was introduced into PSCs for the first time by Xiao et al. (2015). Their results revealed that the strong π–π stacking interaction occurs between GD particles and P3HT which is favorable for the hole transportation and improvement of the cell performance. On the other hand, some GD aggregates exhibit a scattering nature, and thus help to increase the light absorption of the PSCs in the long wavelength range. As high as 14.58% light-to-electricity conversion efficiency was achieved, which is superior to the pristine P3HT-based devices. Though, the devices exhibit good stability and reproducibility yet modifications in the energy level is essential to improve band alignment with perovskites. Taking this into consideration, Jung et al. (2017) have used a cobalt complex, tris (2-(1Hpyrazol-1-yl) pyridine) cobalt (II) di[bis (trifluoromethane) sulfonamide] (Co(II)-TFSI) as a p-dopant in P3HT. This improves the conductivity which leads to a downward shift of the energy levels. This facilitates an efficient charge extraction and transfer from perovskite and considerably improves the device performance to achieve a PCE of 16.28%. Moreover, a flexible device incorporating Co-P3HT exhibits an impressive 11.84% PCE and mechanical stability up to 600 bending cycles. The flexible Co-P3HT device was observed to show better air stability than the Li-doped P3HT (Li-P3HT) device for 40 days. These results suggest that Co (II)-TFSI is an alternative to Li salts to realize high performance in PSCs by incorporating polythiophene derivatives.

4.1.4. PTTA polymer based HTMs

Lin et al. (2017) have reported that even a simple modification with poly tri-arylamine (PTAA) based HTM could avoid the need to use standard HTM and delivers a relatively high open-circuit voltage of 1.08 V and a PCE of 16.5% in a simple planar architecture. Matsui et al. (2016) have synthesized three new polymeric triarylamine derivatives with methyl phenyl ethenyl and diphenyl ethenyl functional groups and has used as HTMs. These materials work without any additives, which also showed to be a detrimental for PSC stability. Polymer V873, containing poly [bis(4-phenyl)-(3,5-dimethylphenyl)amine] main chain with methyl phenyl ethenyl fragments attached to it, when used in PSC showed a PCE of 12.3% without any additives, which is better than the usually used PTAA. Zhou

Please cite this article in press as: Pitchaiya, S. et al., A review on the classification of organic/inorganic/carbonaceous hole transporting materials for perovskite solar cell application. Arabian Journal of Chemistry (2018), https://doi.org/10.1016/j.arabjc.2018.06.006

et al. (2017) have reported about a low temperature processed reduced graphene oxide (r-GO)/PTAA bilayer introduced into the inverted PSCs. This bilayer HTL improved the stability of the device, as the r-GO present in the HTL strongly absorbs near-UV light and the present PTAA material acts as a defect complement for r-GO. The bilayer had the benefit of resulting in larger perovskite grains, thus decreasing grain boundary density and enhancing light harvesting. In addition, the energy level gradient in between the layers at the HTM/perovskite interface effectively inhibited charge recombination and facilitates charge extraction and transport within the device.

The energy level alignment diagram of the device components of PSCs in which (n-i-p and p-i-n) long polymer based HTM used is shown in Fig. 7.

4.1.5. Cross-linked polymer based HTMs

Though the performance and stability of the above PTAA shown are not satisfactory also its cost remains higher so the researchers had to focus on finding some other low cost HTM which led to the introduction of cross-linked polymers. The researchers have made serious efforts to unravel the hygroscopic nature of perovskite materials due to the ease of hydrogen bonding formation between methylamine ions and H_2O. The possibility of incorporating a hydrophobic charge-transporting layer on top of the perovskite layer as a protective barrier can be a promising way to improve device performance and alleviate the stability problem. One attractive approach is to develop cross-linkable HTL that can facilitate efficient hole extraction and simultaneously function as a protective barrier since crosslinked materials have been proven to have good solvent and thermal resistance as well as mechanical durability (Li et al., 2016, 2018).

Li et al. (2016) have studied about a cross-linkable HTM as TCTA-BVP from 4,4′,4″-tris(N-carbazolyl)triphenylamine (TCTA) functionalized with two vinyl benzyl ether groups. This crosslink based HTL exhibits higher hole mobility, better morphological stability and enhanced hydrophobicity than the commonly used spiro-OMeTAD. Their results shows that these materials not only facilitate hole extraction from perovskites but also function as an effective protective barrier. The champion device fabricated using this crosslinked HTL shows an impressive PCE of ~18.3% with negligible hysteresis. More importantly, the crosslinked HTL based devices retained over 80% of its initial PCE, revealing the great potential of utilizing crosslinked HTLs to improve their long-term stability. Zhu et al. (2018) have synthesized an n-type conjugated molecule – (c-HATNA) that can be crosslinked as an electron-transporting layer ETL on top of the desired perovskite. By using a proper dopant to increase its electron transporting property, a high PCE of 18.21% was obtained with moisture and thermal stability without encapsulation. Moreover, this c-HATNA ETL has been used in conjunction with another cross-linkable hole transporting layer, c-TCTA-BVP, to fabricate all crosslinked charge transporting layers for PSCs. More importantly, the device with all-crosslinked CTLs showed an impressive thermal stability in the ambient environment: ~ 70% of its initial PCE was maintained after being heated at 70 °C for 300 h.

The above discussions on various organic polymers and small molecules based HTM results suggested HTM used also affects the stability of the PSC and hence a suitable HTM material has to be identified and used.

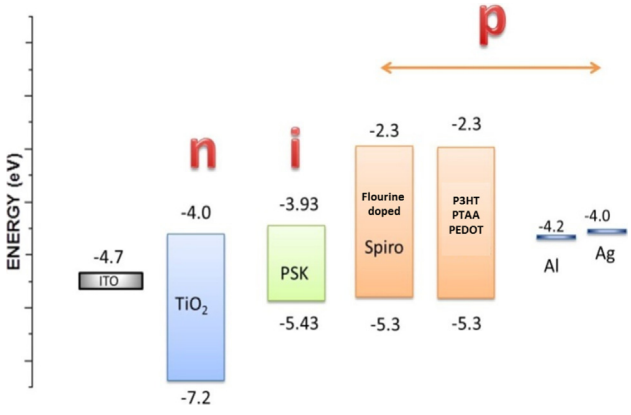

Fig. 7 Energy-level alignment diagram of the device component of perovskite solar cells with (relative to vacuum level) long polymer based HTM in (n-i-p) PSCs.

4.2. *Organic small molecule based HTMs (pyrene/thiophene/porphyrins and carbazoles, etc.)*

Some of the organic small molecules also have the ability to act as a HTM and in this part of the study, the behaviour of the PSCs having small molecule based layer as a HTM is discussed in terms of their photovoltaic properties, device performance and stability (Wang et al., 2017). This small molecules based HTMs can be easily synthesized with high purity and high yield and can be reproduced for industrial production. Its distinct molecular structure with the suitable HOMO energy level value −5.1 to −5.5 eV helps it to be an efficient hole extraction material from the perovskite absorber in PSCs (Saliba et al., 2016). Organic small molecule-based HTMs for solar cell technology was first observed in 1975 by Tang and Albrecht, but the PCE was very low (~1%) (Abdulrazzaq et al., 2013). Thereafter much attention has been paid to develop this cost-effective small molecule-based materials suitable to be used as HTM in PSC device. The available small-molecule based HTMs has been mainly classified as pyrene, thiophene, porphyrins, and carbazoles, etc. (Bakr et al., 2017).

Jeon et al. (2013) have introduced pyrene-core derivative (1-(N,N-di-p-methoxyphenylamine) pyrene) as small molecule HTM. Its efficient charge-transport capability makes it to be a good candidate. They have reported on three different HTMs based on pyrene core and their HOMO value (5.25 eV) is found to be close to that of spiro-OMeTAD (5.22 eV) and using that they have achieved an efficiency of ~12.4% almost equal to that of the efficiency achieved by spiro-OMeTAD (12.7%) and they have also reported that it was more stable than spiro-OMeTAD. Yang et al. (2017) introduced a π-conjugated organic small molecule (4,4′-cyclohexyli denebis[N,N-bis(4-methyl phenyl) benzenamine] (TAPC) which is found to be an efficient HTM to replace PEDOT: PSS in p-i-n-type PSCs with structure, ITO/TAPC-HTM/$MAPbI_3$/PCBM/Ag. This TAPC layer seems to be smooth, uniform, hydrophobic and can be easily deposited through solution casting. The π-conjugation and crystallinity of TAPC makes it to exhibit high hole conductivity without the need for

doping. Further, perovskite material deposited onto TAPC also showed smooth and uniform surface morphology, with an average grain size of ≈310 nm. Their champion device exhibited a PCE of 18.80%, much higher than PEDOT: PSS HTM based devices (12.90%). Also the PSC device exhibited superior stability under ambient conditions than the standard PEDOT: PSS based devices. Their results also indicated that the performance of the devices showed very negligible dependence on the thickness of the TAPC layer.

Thiophene-based small molecule HTMs (2,5-bis(4,4′-bis (methoxyphenyl) aminophen-4″-yl)-3,4-ethylene dioxythiophene) (H101) for PSCs was introduced by Li et al. (2014). The PSC device with thiophene-based molecules as HTM have produced a promising PCE of 10.6% in which when the HTM is doped with cobalt salt the efficiency improved to over 13%, with the best devices matching the value of 13.7% obtained using spiro-OMeTAD doped with the same salt as a reference. The same group have developed films with superior air stability and higher solubility in common solvents compared to H101 which had deeper HOMO levels (H111 and H112 are 5.31 and 5.29 eV, respectively) than H101 (5.16 eV) and they were able to develop them by making some modifications in the thiophene core based molecules and named it as, (2,3,4,5-tetra[4,4′-bis(methoxyphenyl) aminophen-4″-yl]-thio phene (H111) and 4,4′,5,5′-tetra[4,4′-bis(methoxyphenyl) aminophen-4″-yl]-2,2′-bithiophene (H112). The voltage values improved upon doping H101 from 0.97 to 1.05 V matching with the value observed with spiro-OMeTAD (as the HOMO of H101 is –5.16 eV compared to –5.22 eV for spiro-OMeTAD, one expects it to produce a lower V_{OC}) and the FF rose from 0.57 to 0.65 (0.69 for spiro-OMeTAD). This resulted in improved PV performance, from ∼13.8% for H101 to ∼14.7% and 14.9% for H112 and H111, respectively.

Chou et al. (2016) are the first group to develop porphyrin-based HTMs (Y2 and Y2A2) in which two ethynylaniline moieties are bonded to porphyrin core horizontally and the other two alkoxy-phenyl groups are bonded vertically which resulted in very low PCE value. Chen et al. (2017) have reported on using tetra alkoxy-triphenylamine substituted porphyrin-based HTMs and studied the effect of metal ions in the central cavity of the porphyrin ring and they have achieved a PCE of >17% and this device performance seems to be lower than that of the state-of-the-art spiro-OMeTAD existing during that time. Similarly, Lee et al. (2017) have recently employed a series of novel porphyrin derivatives as HTMs namely; PZn-TPA-O (5,10,15,20-tetrakis(4-bromophenyl) porphyrin), PZn-TPA (5,10,15,20-tetrakis(5-bromopyridine-2-yl) porphyrin), PZn-DPPA-O (5,10,15,20-tetrakis(4-bromophenyl) porphyrin zinc(II)) and PZn-DPPA (5,10,15,20-tetrakis(5-bro mopyridine-2-yl) porphyrin zinc(II)). These PZn-DPPA based devices showed a higher PCE value of 18% compared to PZn-TPA based devices and showed much improved air-stability in both doped and un-doped forms compared to spiro-OMeTAD. This study on the structure and properties of porphyrin-based HTMs provides a valuable information for the further development of HTMs in PSCs. The hydrophobic property of PZn-DPPA contributed in enhancing air stability, while the face-on orientation offered relatively high hole-transport. The good hole transporting property of PZn-DPPA even without dopant will be beneficial for future design for dopant-free porphyrin based HTMs. Due to the ease of synthesis, good thermal, optical and photophysical properties, this type of molecules hold great promise for practical application in commercial perovskite solar cells.

Carbazole derivatives have attracted much attention due to their interesting photovoltaic properties such as low cost of its starting material, good chemical and environmental stability, it‘s reactive sites can react with a wide variety of functional groups to fine-tune its electronic and optical properties (Prachumrak et al., 2013). Magomedov et al. (2018) have developed a series of new type of HTMs containing two diphenylamine-substituted carbazole fragments linked by a nonconjugated methylenebenzene unit in PSCs. Their results on the performance of two newly introduced HTMs (V885 and V911) were on a par with spiro-OMeTAD. Chen et al. (2017) designed and synthesized a low-cost carbazole based small molecule material, 1,3,6,8-tetra (N, N-p-dimethoxyphe nylamino)-9-ethylcarbazole through a facile synthetic route. The material was characterized and applied as an HTM for low-temperature processed planar PSCs. Devices based on this new HTM showed PCE of 17.8% which is comparable to that of the available spiro-OMeTAD based devices (18.6%). A simple carbazole-based conjugated enamine V950 was synthesized, fully characterized and incorporated into a PSC by Daskeviciene et al. (2017) which displayed improved efficiency of 18%. They synthesized carbazoles using an extremely simple route from commercially available and relatively inexpensive starting reagents, resulting in lower cost of the final product compared to the commercial spiro-OMeTAD. They have stated that this types of carbazole based HTMs promise to be a commercial viable p-type organic charge conductor to be employed in perovskite solar modules. Kang et al. (2015) reported the synthesis and characterization of novel carbazole-based HTMs with two or three-arm chemical structures, which were linked through phenylene-derived central core units and the PSC fabricated using them achieved a PCE of 14.79%, which is comparable to that of the device with a commercial spiro-OMeTAD (15.23%). Malinauskas et al. (2016), Gratia et al. (2015) have reported about a new type of branched hole transporting material consisting of molecules based on methoxy diphenylamine substituted fluorene and carbazoles, with PSC performance (19.96%) equal to that of spiro-OMeTAD and PTAA. Lu et al. (2017) have used a simple synthesis method and molecular engineering to develop low-cost and star-shaped carbazole based HTMs for highly efficient PSCs. They have designed and synthesized three derivatives of SGT-405(2,7), 18 SGT-410(2,7) and SGT-411 (2,7) via tuning the substitution position from the 2,7 to the 3,6 position of carbazole and used them as HTM in PSC which showed a remarkable PCE of 18.87%, which was better than spiro-OMeTAD (17.71%). Thus all the above results indicate that the carbazole-based transporting materials are a promising class of hole-transporters for PSCs.

5. Classification of inorganic hole transporting materials

Metals such as copper and its derivatives and nickel and its derivatives can play the role as a transporting layer in PSCs. Some of their physical and chemical properties of the selected nickel and copper-based derivatives have been given in Table 3.

Please cite this article in press as: Pitchaiya, S. et al., A review on the classification of organic/inorganic/carbonaceous hole transporting materials for perovskite solar cell application. Arabian Journal of Chemistry (2018), https://doi.org/10.1016/j.arabjc.2018.06.006

Table 3 Material properties of nickel and copper based HTMs used in PSCs.

S. No.	Material property	NiO	Ref. no.	Copper based derivatives					
				CuI	Ref. no.	Cu_2O	Ref. no.	CuSCN	Ref. no.
1.	Dielectric permittivity	10.7	Kurnia et al. (2010)	6.5	Madelung and Madelung (2004)	7.11	Zhu et al. (2011)	10	Dhakal et al. (2011)
2.	Electron mobility (cm^2/V s)	12	Chia-Ching and Cheng-Fu (2013)	100	Giorgi et al. (2013)	200	Korzhavyi and Johansson (2011)	100	
3.	Hole mobility (cm^2/V s)	2.8	Tyagi et al. (2012)	43.9	Chen et al. (2010)	80	Hideki et al. (1996)	25	
4.	Acceptor concentration (1/cm^3)	1.0×10^{18}	Hossain et al. (2015)	1.0×10^{18}	Hossain et al. (2015)	1.00×10^{18}	Lee et al. (2012)	1.0×10^{18}	Hossain et al. (2015)
5.	Bandgap (eV)	3.8	Subbiah et al. (2014)	3.1	Wu and Wang (1997)	2.17	(Hossain et al., 2015)	3.6	(Ahirrao et al., 2011)
6.	CB DOS (1/cm^3)	2.8×10^{19}	Giorgi et al. (2013)	2.8×10^{19}	Giorgi et al. (2013)	2.02×10^{17}	Zhu et al. (2011)	2.2×10^{19}	Dhakal et al. (2011)
7.	VB DOS(1/cm^3)	1.0×10^{19}		1.0×10^{19}	Giorgi et al. (2013)	1.10×10^{19}		1.8×10^{18}	
8.	Electron Affinity (eV)	1.46	(Wu and Wang (1997)	2.1	Hodes (2013)	3.20	Hossain et al. (2015)	1.7	Ahirrao et al. (2011)

5.1. Nickel and its derivatives based HTMs

Nickel oxide (NiO) is one of the most promising HTM with expected stability as it has good optical transparency, prevents electron leakage and has appropriate energy levels (Irwin et al., 2008). NiO layer has a wide band gap and acts as a p-type transporting layer (Jeng et al., 2014) and acts as an electron blocking layer suppressing charge recombination and enhances the hole extraction in solar cells, since the performance of the solid-state PSC device mainly depends on the charge transport (Cui et al., 2014). Among several inorganic HTM used in PSCs, NiO as HTM also has the favorable deep-lying HOMO (valence band edge value) with work function from 5 eV to 5.6 eV (Garcia et al., 2012). NiO acts as a potential HTL with methylammonium lead iodide perovskite and exhibits good hole transfer characteristics and this leads to improved device performance. The inertness of NiO makes it non-corrosive towards ITO substrates and its work function makes NiO a good HTM for PSCs. Initially, Snaith's group used NiO layer as HTL, but they obtained a photoconversion efficiency of $<0.1\%$, due to poor adhesion between perovskite and the NiO layer.

Hu et al. (2014) built an efficient inverted planar PSC using NiO as the hole-collecting layer by using a sequential deposition method. Since NiO has an affinity for carbonaceous species and other contaminants during storage it was treated with UV radiation and this was found to increase the work function of NiO. NiO film thickness optimization and UV-ozone (UVO) treatment improved the efficiency and a PCE of 7.6% with a V_{OC} of 1.05 V was obtained. Li et al. (2015) have deposited $CH_3NH_3PbI_3$ onto planar NiO layer through a spin-coating (8000 rpm) method and built a planar ITO/NiO/$CH_3NH_3PbI_3$/PCBM/BCP/Al (BCP-bathocuproine) device which exhibited an efficiency of 7.9%; they then incorporated a mesoporous NiO layer into the planar device and obtained 9.51% efficiency. They also found that the UVO treatment was beneficial for the device, and the highest V_{OC} they achieved was 1.04 V. These reports clearly showed that NiO is indeed a very promising functional layer in PSCs. Generally, NiO nanocrystals (NiO_{nc}) acts as efficient light–scattering center, which increases the effective optical path length of the device and exhibits a higher transparency than conventional NiO thin films. Zhu et al. (2014) have used sol–gel process to obtain a thin NiO nanocrystalline film and used it in NiO/$CH_3NH_3PbI_3$ solar-cell device. The thin NiO_{nc} film with a faceted and corrugated surface enabled the formation of a continuous and compact layer of well-crystallized $CH_3NH_3PbI_3$. The rough NiO film surface formed by the aggregation of faceted NiO nano scale mono crystals permits the formation of an intimate, large interfacial-area junction with the $CH_3NH_3PbI_3$ film, and this dramatically improved the cell efficiency.

Pitchaiya et al. (2018) have recently reported about the low-cost inorganic nickel sulphide-carbon (NiS-C) composite synthesized using the simple chemical method and has used it as hybrid hole extraction and as a counter electrode material for perovskite ($CH_3NH_3PbI_3$)-based solar cells. They have found that the optimal bandgap of the prepared NiS-C composite material is favorable in achieving the hole extraction property. The surface morphology of the nickel sulphide carbon materials is found to be highly dependent on the

NiS-carbon composition. The perovskite solar cell fabricated using NiS with 20% carbon composition as HTL exhibited a power conversion efficiency of 5.20%. Wang et al. (2014), obtained an efficient charge separation at HTM/perovskite junction by replacing the p-contact with inorganic metal oxide material NiO_x as a mesoscopic layer and NiO_{nc} as a thin capping layer for perovskite. When a mesoscopic electrode is used as charge collector, the sequential deposition method used for depositing the different layers of a PSCs provides better filling of perovskite into the nano-porous pores and more conformal surface coverage on the NiO_{nc} surface. This prevents the direct contact between the n-contact layer (PCBM) with the p-contact material (NiO_{nc} or NiO_x). This $CH_3NH_3PbI_3$ perovskite/NiO heterojunction solar cell exhibited a power conversion efficiency of 9.51% with a higher V_{OC} of 1.04 V and J_{SC} 13.24 mA cm^{-2}. NiO/perovskite films have a very high yield (95%) of PL quenching which shows that the NiO particles not only act as a scaffold layer but have proven to be a very efficient p-type counterpart. Li et al. (2014) developed a hybrid interfacial layer of "compact NiO/meso-Al_2O_3" for an inverted PSC, which led to marked improvement in photovoltaic performance. The hybrid interfacial layer made of an ultrathin NiO compact layer (10–20 nm) and a thin meso-Al_2O_3 layer (90 nm) exhibits "dual blocking effect". The interfacial recombination loss could be sufficiently minimized. Moreover, ultrathin NiO and transparent meso-Al_2O_3 as a hybrid interfacial layer guarantees an excellent optical transmittance, which can minimize the optical loss in NiO based perovskite sensitized solar cells. This is substantial progress in NiO based PSCs, in view of the great challenge on a critical balance between high optical transmittance and efficient electrical blocking at the interface.

A mesoscopic PSCs device using a quadruple-layer architecture consisting of inorganic metal oxide in combination with carbon counter electrode was constructed by Cao et al. (2015). Here both the NiO and Al_2O_3 layers of the fabricated cell act as a spacer layer to separate TiO_2 and the carbon counter electrode. A reduced interfacial charge recombination was observed in quadruple-layer mesoscopic PSCs containing a NiO layer when compared to the device structure that uses only Al_2O_3 as a spacer layer. As a result, a higher PCE of 15.03%, J_{SC} of 21.62 mA cm^{-2} and FF of 76% were achieved. Moreover, quadruple-layer mesoscopic PSC devices containing a NiO layer exhibit good stability which contributes to highly efficient PSCs. When compared to the performance of PEDOT: PSS/spiro-OMeTAD and other organic HTMs, the performance of NiO in PSCs is still not satisfactory due to a lower fill factor and reduced short-circuit current density even though there is a significant improvement in the V_{OC}. Although ionic radius of copper is slightly larger than that of nickel, Kim et al. (2015) observed that upon incorporating 5 at% of Cu in Ni there is a reduction in the NiO_x lattice parameter. They fabricated 5 at% Cu doped NiO_x based PSCs which exhibited a PCE of 15.4% with V_{OC} of 1.11 V, J_{SC} of 19.01 mA cm^{-2} and FF of 73% which is substantially better than the performance of PEDOT: PSS based devices. Similarly, Tvingstedt et al. (2014) have stated that, for a good photovoltaic material combination the absorber should display strong PL quenching due to beneficial induced charge transfer. Their work on Cu: NiO_x $MAPbI_3$ films suggest that there is a great degree of PL quenching indicating enhanced hole collection and transport efficiency, and exhibit good electrical conductivity. Thus, the good performance of Cu: NiO_x $MAPbI_3$ film based solar cells shows the promising potential of Cu: NiO_x which can be used in perovskite tandem solar cells. Park et al. (2015) prepared NiO film with good optical transparency through a pulsed laser deposition method and used it as a p-type transport layer. The PSCs constructed using the developed nanostructured NiO film exhibited a high PCE of 17.3%. To gain more insight into how the hole extraction property depends on the morphology of NiO layer, the dark current and recombination lifetime of devices were studied. Compared to the "nanostructured" film, the "disordered" film showed a higher dark current due to its loosely packed porous microstructure, which caused an insufficient electron blocking/hole extraction.

The device structure, thickness of the HTMs used, the IPCE and photovoltaic parameters of the PSCs fabricated using Nickel based HTMs are given in Table 4. The energy level alignment diagram of the PSCs device elements in the n-i-p and p-i-n device configuration is shown in Figs. 8 and 9 respectively.

5.2. ***Copper and its derivatives based HTMs*** *(CuI/Cu_2O/CuO/$CuCrO_2$/$CuGaO_2$)*

Inorganic copper based p-type semiconductors such as CuI/Cu_2O/CuO/$CuCrO_2$/$CuGaO_2$ are considered to be potential hole conductors to be used in PSCs. They have been already used in dye-sensitized and quantum dot solar cells. Also, their interesting photovoltaic properties such as wide band gap high conductivity, and simple synthesizing methods (solution-based) at relatively low cost have made them worthy HTMs in PSC technology.

Christians et al. (2014) have fabricated PSCs using CuI as an HTL deposited by drop casting method. The cells exhibited an efficiency of 6%. They concluded that though CuI provides a higher fill factor than spiro-OMeTAD, the efficiency is still lower which can be attributed to the higher recombination rate. As the perovskite layer used for planar device architecture is relatively thin, CuI can easily form short-circuits between the electrode and counter electrode through pinholes in the perovskite layer. Huangfu et al. (2015) have stated that a very thin mesoporous layer cannot absorb enough perovskite, and so produces a narrow depletion region which cannot separate electron-hole pairs efficiently. But a thicker mesoporous layer leads to large recombination of the injected electrons in the TiO_2 conduction band with the holes in the perovskite. The fabricated solar cells showed a very low V_{OC} due to (i) low charge carrier diffusion length and (ii) the cavitation in CuI layer, which creates paths that decrease the shunt resistance and increase the series resistance. Sepalage et al. (2015) have used copper iodide deposited by doctor blade technique and the surface was found to be rough and showed gaps between particles. There was no variation in the device with respect to change in the CuI film thickness, but a comparatively high efficiency was obtained with changes in the texture of the perovskite film. They also observed that the magnitude of the charge separation is smaller at the perovskite/CuI interface when compared to the perovskite/spiro-OMeTAD interface. Further, Chen et al. (2015) have synthesized CuI transport layer using the low-cost solution process method to replace the commonly used PEDOT: PSS in inverted PHJ PSCs and

Please cite this article in press as: Pitchaiya, S. et al., A review on the classification of organic/inorganic/carbonaceous hole transporting materials for perovskite solar cell application. Arabian Journal of Chemistry (2018), https://doi.org/10.1016/j.arabjc.2018.06.006

Table 4 Photovoltaic characteristics of perovskite solar cells with inorganic nickel based HTMs.

S. No	Device gestalt	Structure type	Inorganic nickel based HTLs		IPCE (response range) (nm)	Photovoltaic parameters				Ref.
			Method	Thickness		V_{OC} (V)	J_{SC} (mA/cm^2)	FF (%)	η (%)	
1.	FTO/NiO/PSK/PCBM/BCP/Au	Planar p-i-n	Sputtering	50–100 nm	400–800	1.1	15.17	59	9.84	Cui et al. (2014)
2.	ITO/NiO/PSK/PCBM/Li-F/Al	Mesoscopic p-i-n	Pulsed laser deposition	100 nm	300–800	1.03	19.2	78	15.3	Park et al. (2015)
3.	FTO/c-TiO_2/M-TiO_2 + PSK/Al_2O_3 + PSK/NiO + PSK/carbon	Multilayered n-i-p	Screen printing technique	800 nm	350–750	0.9	21.62	76	15.03	Cao et al. (2015)
4.	ITO/Cu doped NiO_x/PSK/PCBM + C_{60}-bis surfactant/Ag	Planar n-i-p	Spin coating	300 nm	300–800	1.11	18.75	72	14.98	Kim et al. (2015)
5.	FTO/NiO/PSK/PCBM/Au (NiO – nanocrystals)	Planar p-i-n	Spin coating	40 nm	350–800 nm	0.88	16.27	63.5	9.11	Zhu et al. (2014)
6.	TiO_2/ZrO_2/NiO/C + PSK	Multilayered n-i-p	Doctor blade	480 nm	460–800 nm	0.917	21.36	76	14.9	Xu et al. (2015)
7.	FTO/NiO/Meso-Al_2O_3/PSK/PCBM/BCP/Ag	Mesoscopic p-i-n	Spray pyrolysis	30–50 nm	300–800	1.04	18	72	13.5	Li et al. (2014)
8.	ITO/NiO_x/PSK/ZnO/Al	Planar p-i-n	Doctor blading	80 nm	300–800	1	21	76	16.1	You et al. (2015)
9.	ITO/sputtered NiO_x/NiO nanocrystals/PSK/PCBM/BCP/Al	Mesoscopic p-i-n	Sputtering	10 nm	350–800	0.96	19.8	61	11.6	Wang et al. (2014)
10.	ITO/NiO/PSK/PCBM/Ag	Planar p-i-n	Spin coating	240 nm	300–800	1.02	20	62	12.7	Park et al. (2015)
11.	ITO/NiO_x/PSK/PCBM/BCP/Al	Planar p-i-n	Spin casting	10 nm	300–800	0.92	12.43	68	7.8	Wang et al. (2014)
12.	FTO/c-TiO_2/m-TiO_2/PSK + NiO(composite)/Au	Planar n-i-p	Spin coating	400 nm	300–800	0.82	26.41	56	12.14	Wang et al. (2016)
13.	FTO/c-TiO_2/m-TiO_2/NiO/PSK/Carbon	p-i-n	Screen printing	1 μm	400–800	0.89	18.2	71	11.4	Liu et al. (2015)
14.	ITO/NiO_x/NiO nanocrystals/PSK/PCBM/BCP/Al	Mesoscopic p-i-n	Spin coating	100 nm	400–800	1.04	13.24	69	9.51	Wang et al. (2014)
15.	ITO/NiO/PSK/PCBM/Au	Planar p-i-n	Spin coating	10.2 nm	300–800	0.94	13.1	47	7.6	Hu et al. (2014)

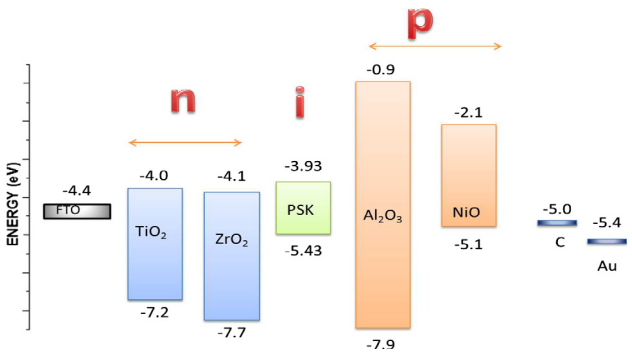

Fig. 8 Energy-level alignment diagram of the device components of perovskite solar cells in which (relative to vacuum level) NiO as HTMs in (n-i-p).

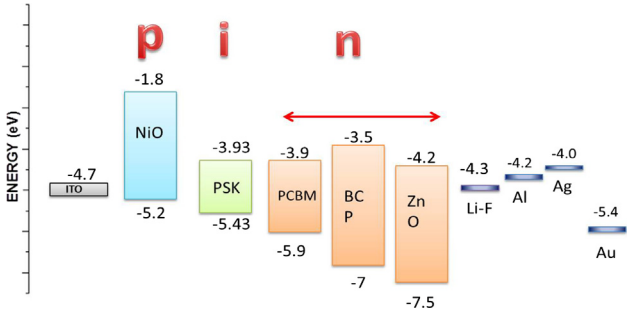

Fig. 9 Energy-level alignment diagram of the device components of perovskite solar cells in which (relative vacuum level) NiO is used as HTM in (p-i-n) PSCs.

observed higher performance and improved stability. The hydrophobic nature and ambient stability of CuI dramatically improved the stability of inverted PHJ PSCs. The CuI film exhibits PL quenching more efficiently than that of PEDOT: PSS films which demonstrate that CuI can be used as an HTL replacing PEDOT: PSS. The root means square (RMS) roughness was found to be increased to 8.6 nm after being covered with CuI layer. The results showed higher V_{OC} due to the lower HOMO energy level and higher J_{SC} due to more efficient charge transport process and/or light harvesting. Liu et al. (2016) have used Cu_2O and CuO as HTMs in PSCs which showed significantly enhanced PCE of 13.35% and 12.16% respectively. The PL results showed that the higher PL quenching for the Cu_2O and CuO layers, which can make them to play the role of HTMs effectively and can be a suitable alternative for the replacement of unstable PEDOT: PSS.

Recently, Qin et al. (2017) introduced a novel copper-chromium ($CuCrO_2$) binary metal oxide as HTM synthesized using low-temperature solution-process method for PSC. The energy levels and phase composition of this binary metal oxide $CuCrO_2$ can be modulated by using different copper acetylacetonate/chromium acetylacetonate. Unlike copper oxides, the copper-chromium binary metal oxide films have wide band gap of around 3.1 eV, as well as suitable energy levels for hole-transporting. As a result, PSCs with this low-temperature solution processed copper-chromium binary metal oxide HTL have achieved high PCE of 17.19% on the glass and 15.53%, which is a significant enhancement when

Table 5 Photovoltaic characteristics of perovskite solar cells using inorganic copper based HTMs.

S. No.	Device gestalt	Structure type	Inorganic copper based HTLs		IPCE (response range) (nm)	Photovoltaic parameters				Ref.
			Method	Thickness		V_{OC} (V)	J_{SC} (mA/cm^2)	FF (%)	η (%)	
1.	FTO/b-TiO_2/m-TiO_2/PSK/CuI/Au	Mesoscopic n-i-p	Doctor blading	1.5–2 μm	400–800	0.55	17.8	62	6.0	Christians et al. (2014)
2.	FTO/TiO_2/PSK/CuI/Au	n-i-p	Spray coating	17.5 μm	400–770	0.646	21	33	4.5	Huangfu et al. (2015)
				24.8 μm		0.640	22.6	39	5.6	
				28.8 μm		0.698	22.1	33	5	
				36.9 μm		0.693	22.7	31	4.8	
3.	FTO/bl-TiO_2/PSK/CuI/graphite/Cu-tape	Planar n-i-p	Doctor blading	300 nm	330–800	0.78	16.7	57	7.5	Sepalage et al. (2015)
4.	FTO/CuI/PSK/PCBM/Al	n-i-p	Spin coating	43 nm	400–800	1.04	21.06	62	13.58	Chen et al. (2015)
5.	ITO/Cu_2O/PSK/C_{60}/B phen/Ag	n-i-p	Electro deposition	4–5 μm	350–780	0.88	18.03	61	9.64	Liu et al. (2016)
6.	ITO/CuO_x/PSK/PCBM/ZnO NPs/Al	n-i-p	Spin coating	–	350–800	1.03	22.42	76	17.43	Yu et al. (2016)
7.	ITO/CuI/PSK/PCBM/Ca-Al	n-i-p	Spin coating	15–47 nm	300–780	1.07	16.52	75.5	13.35	Zuo and Ding (2015)

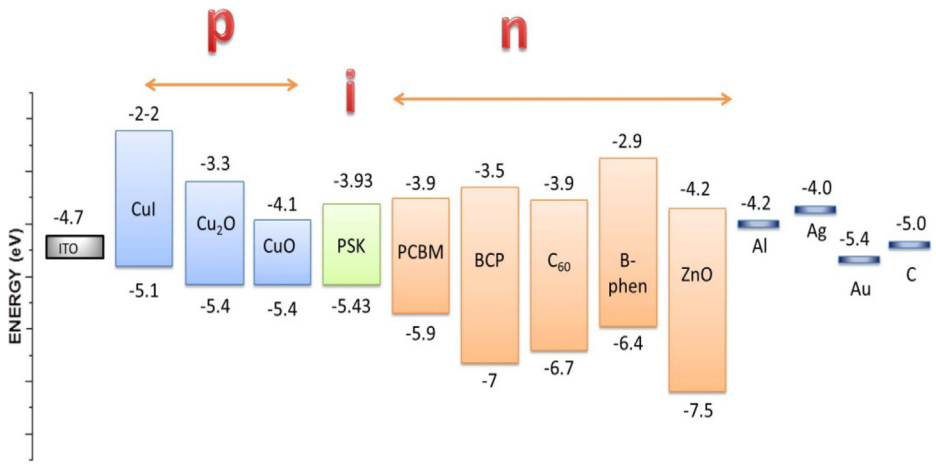

Fig. 10 Energy-level alignment diagram of the device component of perovskite solar cells in which (relative to vacuum level) Copper based (CuI/Cu_2O/CuO) HTMs in (p-i-n) PSCs.

compared to mono-metal oxide-based devices. Zhang et al. (2017) have fabricated an efficient PSC using solution-processed $CuGaO_2$ as HTL and have acheived an impressive PCE of 18.51% and have found that the stability of these devices to be much better compared to other inorganic HTMs. Galatopoulos et al. (2017) have fabricated PSCs by replacing the most commonly used organic PEDOT: PSS with inorganic based Cu: NiOx and CuO HTLs and the PCE values increased from 8.44% to 11.45% and 15.7% respectively. Thus, using copper and its derivatives as HTMs have shown an efficient PCE and improved stability crisis in PSCs could be an alternative to the high cost and unstable organic HTMs. The device structures, method and thickness of the HTMs used, the IPCE and photovoltaic parameters of the PSCs fabricated using copper-based HTMs are given in Table 5. The energy level alignment diagram of the PSCs device elements in the p-i-n device configuration is shown in Fig. 10.

5.3. ***p-type semiconductor HTMs*** *(copper phthalocyanine (CuPc) & cuprous thiocyanate (CuSCN))*

Copper phthalocyanine (CuPc) – being a derivative of copper is found to be one of the alternative HTM in PSCs due to it's low-cost, high hole mobility ($\sim 10^{-3} - 10^{-2}$ cm^2 V^{-1} s^{-1}), stability and long exciton diffusion length. Considering all the superior photovoltaic properties of CuPc, Kumar et al. (2015) have fabricated solid-state PSCs by employing copper phthalocyanine as HTM. The best cell demonstrated a J_{SC} of 16.3 mA cm^{-2}, V_{OC} of 0.75 V and PCE of 5%. The fabricated cells show relatively large differences between the two charge acceptor levels (conduction band of titania and the LUMO level of CuPc). The fill factor of the cell was relatively small and this limits the cell efficiency when compared to the cells made with spiro-OMeTAD as HTMs. Low-temperature printable carbon cathode based PSCs was introduced for the first time with interfacial engineered dopant-free, nanorod like copper phthalocyanine to facilitate charge transportation (Zhang et al., 2016). By incorporating CuPc nanorods as hole–selective contact material, together with the printable low temperature processed carbon as a cathode material, a high-power conversion efficiency of 16.1% was obtained successfully. $CH_3NH_3PbI_3$/CuPc/C solar cell exhibited a high FF of 74%, which may be due to the better contact of the cathode with CuPc and low charge transport resistance. There was no significant increase in photocurrent due to the back reflection from gold (Au) cathode. In CuPc based PSCs, light transmitted through the perovskite layer could be absorbed by the thin CuPc nanorods layer and the relatively rough surface of CuPc nanorods might also act as a scattering layer blocking the transmitted light to a large extent. Thereby, the light transmitted through the layers of $CH_3NH_3PbI_3$ and CuPc which get reflected from the back electrode is found to be much reduced. Nanorod–like shape CuPc exhibits stronger quenching effects (~95%), which indicate that CuPc nanorods are more effective in hole extraction owing to the high interfacial film quality with intimate contact with the perovskite. Chavhan et al. (2014) have demonstrated the viability of using solution processed CuSCN films as hole selective contact in PSCs using a planar heterojunction and have acheived PCE of 6.4%.

Wang et al. (2018) have developed an efficient and stable doped Copper Phthalocyanine based HTM, (F4-TCNQ-doped TS-CuPc) to fabricate high-performance PSCs. p-type conductivity was realized in TS-CuPc and F4-TCNQ with obviously improved film conductivity and hole mobility. The doping also resulted in a band bending of TS-CuPc with a high HOMO level of 5.3 eV, which is beneficial for hole extraction in corresponding PSCs. The TSCuPc:F4-TCNQ composite film presented good stability because of the almost neutral precursor solution, which avoided the electrode erosion. More importantly, F4-TCNQ-doped TS-CuPc could be employed as an HTM not only in the p–i–n structure but also in the n–i–p structure PSCs. Particularly, a champion n–i–p structured device with a PCE as high as 20.16% was obtained. The developed organic small molecule semiconductor of TS-CuPc provides the diversification of HTMs in planar PSCs. It will stimulate the researchers to develop other organic-based HTMs for fabricating high-performance PSCs. Ito et al. (2014) studied the behavior of HTL against humidity in PSCs. The PSCs with spiro-OMeTAD had strong humidity effects whereas the PSCs with cuprous thiocyanate as an HTM exhibited good coverage against humidity. Hence, it was understood that the humidity effect in PSCs should be

associated to the HTMs rather than perovskite materials. Solution-processed inorganic p-type semiconductors have been proposed as alternatives to PEDOT:PSS owing to their relative low cost, greater stability and potential for implementation in a hybrid tandem structure. Low temperature solution processed, thin and smooth CuSCN films can be used as effective bottom HTL in planar heterojunction p-i-n solar cells (Zhao et al., 2015). CuSCN based planar heterojunction p-i-n solar cells consistently show a PCE of 10.8% with negligible hysteresis. CuSCN based PSCs show strong PL quenching implying that charge transfer occurs efficiently at the CuSCN-perovskite interface. Favorable energy level combination at CuSCN/perovskite interface increases the V_{OC} substantially by 0.23 V when compared to PEDOT:PSS HTL. The solar cells with CuSCN based HTL exhibit 1% higher PCE than the solar cells with PEDOT:PSS and this is used as HTL, due to significant increase in V_{OC} despite slight decrease in FF and J_{SC}. Furthermore, Ito et al. (2014) for the first-time fabricated planar PSCs with CuSCN as HTL by sequential deposition method and the cell exhibited a PCE of 11.96%. They have reported that cell surface should be smooth with less pinholes in the perovskite layer and such a smooth perovskite layer may block the short circuit between ETL and HTL layers (i.e. TiO_2 and CuSCN). Due to partial short circuits in the planar solar cells fill factors reduces. Similarly, Qin et al. (2014) have demonstrated the use of an effective inorganic p-type CuSCN-HTM synthesized using solution-process deposition method. The presence of CuSCN leads to an improvement in the overall efficiency to 12.4% through a 65% increase in J_{SC} and 9% increase in V_{OC}. The high short circuit current and IPCE values indicate efficient charge extraction and collection from the excited perovskites by TiO_2 and CuSCN, respectively. CuSCN can extract hole carriers efficiently while blocking electrons at the CuSCN/perovskite interface. The high transparency of $CH_3NH_3PbI_3$ improves light absorption and helps in generating higher photocurrent in the device. The optimized CuSCN derived PSCs exhibited a PCE of 16% increase in V_{OC} to 1.07 V. This can be attributed to better energy alignment or reduced resistance at the HTL/perovskite interface, which minimizes the potential loss across the HTL/perovskite interface and increases the built-in potential of the device to a value more than PEDOT:PSS. High transmittance is another important reason for improved J_{SC} in the device (Jung et al., 2015). It is noteworthy to mention that the morphology and crystallinity of perovskite layers in both CuSCN and PEDOT:PSS HTLs are quite similar and so the higher V_{OC} and J_{SC} of the CuSCN based device is mainly attributed to a better energy level matching at the CuSCN/perovskite interface which leads to better charge extraction and transport. CuSCN film as HTL was used in inverted PSCs (Ye et al., 2015). They have discussed the feasibility of various deposition methods in obtaining high–quality perovskite films on top of a rough CuSCN layer by a one-step, fast-deposition crystallization method and have obtained an efficiency of 16.6% with CuSCN as HTM. Compared to the perovskite film present on top of a rough CuSCN layer prepared by a conventional two-step sequential deposition process, the film prepared by one-step process had lower surface roughness and the interface contact resistance between the perovskite layer and the selective contacts was small, which resulted in higher PCE (16.6%). Jung et al. (2016) have fabricated PSCs using low temperature

Table 6 Photovoltaic characteristics of perovskite solar cells using p-type semiconductor based HTMs.

S. no.	Device gestalt	Structure type	p-type semiconductor based HTLs		IPCE (response range) (nm)	Photovoltaic parameters				Ref.
			Method	Thickness		V_{OC} (V)	J_{SC} (mA/cm^2)	FF (%)	η (%)	
Copper phthalocyanine (CuPc) based HTMS										
1.	ITO/TiO_2/PSK/CuPc/Au	Planar n-i-p	Vacuum deposition	200 nm	350–800	0.75	16.3	40	5	Kumar et al. (2015)
2.	ITO/c-TiO_2/m-TiO_2/PSK/CuPc nanorods/carbon	Mesoscopic n-i-p	Doctor blade	< 500 nm	400–800	1.05	20.8	74	16.1	Zhang et al. (2016)
Cuprous thiocyanate (CuSCN) based HTMS										
1.	TiO_2/PSK/CuSCN/Au	Mesoscopic n-i-p	Doctor blading	–	400–800	0.63	14.5	53	4.86	Ito et al. (2014)
2.	ITO/CuSCN/PSK/C_{60}/BCP/Ag	n-i-p	Electro deposition	57 nm	350–800	1	21.9	75.8	16.6	Ye et al. (2015)
3.	ITO/CuSCN/PSK/PCBM/BiS-C_{60}/Ag	Planar heterojunction	Spin coating	40 nm	400–800	1.07	19.6	74	15.6	Jung et al. (2015)
4.	FTO/TiO_2/PSK/CuSCN/Au	Mesoscopic n-i-p	Doctor blading	600 nm	450–800	1.02	19.2	58	12.4	Qin et al. (2014)
5.	TiO_2/PSK/CuSCN/Au		Doctor blading	–	400–800	0.96	18.23	68	11.96	Ito et al. (2014)
6.	TiO_2/Mixed halide PSK/CuSCN/Au	Planar n-i-p	Drop casting	500 nm	300–850	0.72	14.4	61.7	6.4	Chavhan et al. (2014)
7.	ITO/CuSCN/PSK/PCBM/LiF-Ag	n-i-p	Spin coating	13 nm	430–620	1.06	15.02	65.4	10.8	Zhao et al. (2015)

solution-processed CuSCN as the inorganic HTL, which possesses a highly stable crystalline structure and is robust even at high temperatures. The fabricated cell delivers a PCE of 18.0%. Thus, the hydrophobic copper based derivatives CuPc and CuSCN materials act as an HTM as well as an interlayer which prevents the perovskite devices under ambient conditions.

The device structure, thickness of the HTMs used, the IPCE and photovoltaic parameters of the PSCs fabricated using CuPc and CuSCN as HTMs are given in Table 6. The energy level alignment diagram of the PSCs device elements in the n-i-p device configuration for p-Type semiconductor (CuPc/CuSCN) based HTMs is shown in Fig. 11.

5.4. *Transition metal oxide based interfacial/HTMs* (MoO_x/VO_x/V_2O_x/WO_x)

The acidic (pH ~ 1) and hygroscopic properties of an organic material always result in a dramatic degradation of the PSCs in ambient conditions and this has made way for the researchers to focus on transition metal oxides such as MoO_3, V_2O_5, WO_3, etc. which have been successfully demonstrated as, as a dopant and as a material for the HTL due to their enhanced stability in PSCs and also due to their high transparency, high work function, smooth surface, high conductivity, and easy solution based synthesis process (Qian et al., 2015).

5.4.1. *Molybdenum oxide (MoO_3) as interfacial/HTM layer*

Among the transition metal oxides, MoO_3 has received great attention because of its high transmittance, non-toxicity, and high work function. Hu et al. (2014) have developed a facile method to synthesis the solution processed MoO_3 monolayer and e-MoO_3/PEDOT: PSS bilayer HTL for polymer solar cells based on P3HT: $PC_{61}BM$. The effect of MoO_3 based HTLs on the device performance are found to be greatly influenced by the surface energy which is caused by the MoO_3 crystal size, the light absorbed, and the exciton generation rate which is related to the composition and thickness of the HTL. As a result, an ultrathin evaporated e- MoO_3 combined with PEDOT: PSS bilayer enhanced the light absorbed and the exciton generation rate in the active layer, consequently leading to a further optimized PCE of 3.98% for P3HT: PC61BM and 7.10% for PBDTTT-C-T: $PC_{71}BM$. Moreover, this

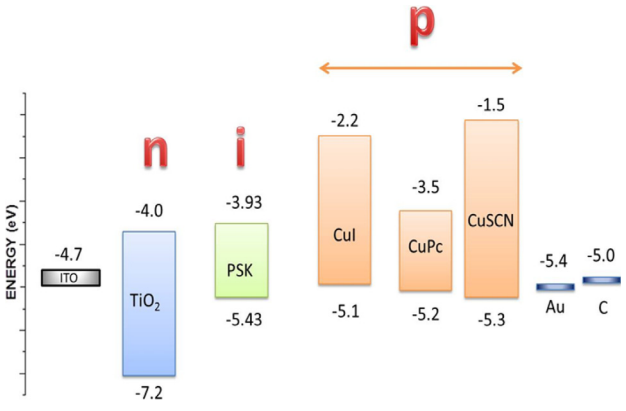

Fig. 11 Energy-level alignment diagram of the device component of PSCs with (relative to vacuum level) p-type Semiconductor (CuPc/CuSCN) based HTMs in (n-i-p) PSCs.

e- MoO_3/PEDOT: PSS also improved the stability of the devices because the MoO_3 not only can prevent the moisture and oxygen attacking but also protect ITO from corrosion caused by the acid PEDOT: PSS. Jiang et al. (2016) have carried out a similar work by simply incorporating the MoO_x powders into the PEDOT: PSS aqueous dispersion and the device showed good performance with a PCE of 15.79% and FF of 75.4%.

Yixin Zhao and Zhu (2014) have used a combination of a thin layer of molybdenum oxide and aluminum as the top-contact structure for extracting photo-generated holes from PSCs in which MoO_x is deposited by thermal evaporation. They could achieve a device efficiency of 11.4%. Hou et al. (2015) have found that the incorporation of the MoO_3 layer in PSCs does not affect the growth of PEDOT: PSS but dramatically improves the PCE and stability of the devices. The device shows a PCE of 12.78%, which is improved by about 30% when compared to the reference device based on pristine PEDOT: PSS. Moreover, the use of PEDOT: PSS as HTM results in a considerable cost reduction, when compared with doped spiro-OMeTAD. The improvement is attributed to the increase in hole collection efficiency of the MoO_3 layer along with PEDOT: PSS HTM. A maximum PCE of 14.87% was obtained for the device, which is among one of the highest PCE reported in inverted PHJ PSCs. Jeng et al. (2014) have used MoO_x:PEDOT: PSS composite film as the HTL in a polymer solar cell to take advantage of both the high conductivity of PEDOT: PSS and the ambient condition stability of MoO_3, and eventually both PCE and stability were found to have improved.

5.4.2. *Vanadium oxide (VO_x/V_2O_x) as interfacial/HTM*

Vanadium oxide is found to be a promising HTMs in PSCs due to it's low-cost, high ambient stability, optimal optical and electrical properties. Taking this strategy into consideration, Cong et al. (2017) have reported a facile way to prepare a vanadium oxide hydrate ($VOx{\cdot}nH_2O$) based HTL for PSCs. They have also reported about short-time thermal annealing of vanadyl acetylacetonate (VO (acac)$_2$) layer and the PSCs based on $VO_x{\cdot}nH_2O$ (H_2O_2-UVO) layer yielded an average PCE of 7.97% with high stability. The PCE is improved by ~32% when compared to the devices with the VO_x layers and is superior to the device with a conventional PEDOT: PSS layer. Thus, the $VO_x{\cdot}nH_2O$ (H_2O_2-UVO) HTM layer reported in this work can be considered as a promising alternative to the conventional PEDOT: PSS layer for high-performance and cost-effective PSCs. Peng et al. (2016) have used inorganic vanadium oxide (V_2O_x) as an efficient interfacial material in perovskite heterojunction cells for achieving improved band alignment and device performance. Solution-processed V_2O_x is incorporated in the PEDOT: PSS/perovskite interface, and a bilayer structure consisting of V_2O_x and PEDOT: PSS acts as the HTL in the inverted PSCs. A PCE of 17.5% with nearly free hysteresis and a stabilized efficiency of 17.1% have been acheived. Their work demonstrates that the novel bilayer material acts as an excellent hole extraction layer in inverted perovskite devices, since V_2O_x affects the interface properties, including surface energy as well as optical and electrical properties.

Lou and Wang (2017) introduced a facial route to deposit solution processed TMOs (MoO_3, GeO_2, V_2O_5 and CrO_3)

interfacial layers by dissolving commercial TMO powder into the deionized water. All the interfacial layers were fabricated and utilized as the HTL. In particular, V_2O_5 film exhibited the highest work function of 5.2 eV and the best hydrophobicity with a contact angle of 77.2° among the four TMO materials. The V_2O_5 based device exhibited a PCE of 13.2%. Furthermore, the composite HTL (by mixing PEDOT:PSS and TMOs) based PSCs demonstrated significantly improved PCE and cell stability when compared with pristine PEDOT: PSS based devices. Devices using the optimized composite film (PEDOT:PSS + V_2O_5) obtained a maximum PCE of 18.03%. The preparation process of MoO_3, GeO_2, V_2O_5 and CrO_3 aqueous solution is quite simple and ecofriendly without any toxicity.

5.4.3. Tungsten oxide (WO_3) as HTM

Tungsten oxide (WO_3) has been employed as hole injection layer in organic light-emitting diodes to reduce the injection barrier at the polymer/electrode interface and lead to higher device performance. In the case of PSCs, WO_3 film can also significantly reduce the series resistance and improve the fill factor in conventional, tandem, and inverted PSCs. Xu et al. (2013) have prepared the (WO_3) buffer layer on an ITO electrode by solution processing from tungsten (VI) isopropoxide solution and then annealed at 150 °C. The solution-processed WO_3 layer is highly transparent in the visible range and shows an effective hole collection property. Thus, this s-WO_3 as HTM layer shows high hole mobility and high light transmittance and showed enhanced performance (6.36%) in comparison with the PEDOT: PSS modified devices. This work gives a new option for the selection of the solution-processed anode buffer layer in designing higher efficiency and more stable PSCs. The energy level alignment diagram of the device components of PSCs in which $MoO_x/VO_x/V_2O_x/WO_x$ are used as interlayer/HTMs (p-i-n) and are shown in Fig. 12. By using transition metal based HTMs as the interfacial layers, an enhanced efficiency and improved stability can be achieved, which cannot be readily achieved with organic interfacial materials. All the above-discussed results and the fundamental insights could be useful in the development of achieving high efficiency and long-term stable PSCs devices at low cost.

From this review on HTM in PSCs, it has been clearly recognized that interfacial engineering plays a critical role in cell performance. It has also been stated that the open circuit voltage is dependent on the ionization potential of the HTMs.

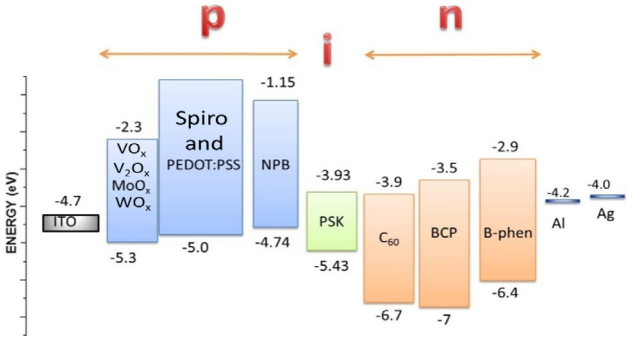

Fig. 12 Energy-level alignment diagram of the device components of PSCs in which (relative to vacuum level) transition metal oxide based interlayer/HTMs is used in (p-i-n) PSCs.

The device structures, thickness of the HTMs used, the IPCE and photovoltaic parameters of the PSCs fabricated using transition metal oxide as HTMs is given in Table 7. Energy-level alignment diagram of the device components of PSCs in which (relative to vacuum level) transition Metal Oxide ($MoO_x/VO_x/WO_x$) based interlayer/HTMs are used in HTL (p-i-n) are shown in Fig. 12.

6. Classifications of carbonaceous hole transporting materials (carbon/graphene oxide/reduced graphene oxide)

Initially, carbon was used as an electrode in promising low-cost PSC photovoltaic devices for better stability. Then it was considered for making hole-conductor-free cells possible and it is also considered as an ideal material to replace the high-cost Au - back contact in PSCs. Though carbon in PSCs is being used as an electrode, its dual role invoked researchers to focus on carbon materials to replace high cost, unstable HTMs. Yang et al. (2014) have reported about the dual role of carbon as a hole acceptor and as a conductive electrode to transport holes (HTL). Further carbonaceous materials such as graphene oxide, reduced-graphene oxides and carbon nanotubes (SWCNTs & MWCNTs) are being used as HTMs in PSCs. The reason for carbonaceous materials to be effective HTMs are its low cost good connectivity and has the unique property of exhibiting good mechanical performance and adhesion to the film which will reduce the interface resistance in solar cells. Also, its approximate work function of 5.0 eV makes it an ideal material to replace the role of HTMs in PSCs (Yang et al., 2014). In addition, carbon-based materials can be easily prepared by simple techniques such as spin coating, the doctor blade method, inkjet printing and the rolling transfer method (Wei et al., 2014; Chen et al., 2014). To enhance the stability, reduce the cost and for improved performance of conventional PSCs, carbonaceous materials will be the effective material which can be a suitable replacement for organic small molecules and long polymer HTMs (Rajeswari et al., 2017; Aitola et al., 2016).

6.1. Hole-transport-free based carbon HTMs

Zhou et al. (2014) have discussed the effect of thickness of carbon film on the electrical conductivity of carbon layer. As the thickness of the carbon layer is increased from 2 to 20 μm, the device showed a significant increase in efficiency which increased from 2 to 6.9%, and this has been attributed to reduced square and series resistance of the device. They also modified the thin film structure by sandwiching active perovskite ($CH_3NH_3PbI_3$) layer between n-type ZnO which acts as an ETL and carbon electrode which acts as hole selective layer ($ZnO/CH_3NH_3PbI_3/C$ PHJ-PSCs) and have achieved PCE up to 8%. This carbon-based hole selective layers are of low cost and are of simple architecture. The facile fabrication process at low temperature without using high vacuum is a promising criterion for future production of all flexible PSCs. The use of a low-cost carbon material prepared at low temperature on top of $CH_3NH_3PbI_3$ without destroying the structure of perovskites offers numerous possibilities to choose materials and optimize the structure of the device and achieve good efficiency.

Please cite this article in press as: Pitchaiya, S. et al., A review on the classification of organic/inorganic/carbonaceous hole transporting materials for perovskite solar cell application. Arabian Journal of Chemistry (2018), https://doi.org/10.1016/j.arabjc.2018.06.006

Table 7 Photovoltaic characteristics of perovskite solar cells using MoO_x, GeO_2, & V_2O_5 and CrO_3 (as an interlayer) as HTMs.

S. no.	Device gestalt	Structure type	MoO_x & V_2O_5 (as an interlayer) based HTLs		IPCE (response range) (nm)	Photovoltaic parameters				Ref.
			Method	Thickness		V_{OC} (V)	J_{SC} (mA/cm^2)	FF (%)	η (%)	
1.	TiO_2/PSK/spiro/MoO_x/Al	Planar n-i-p	Thermal evaporation	10 nm	300–800	0.993	20.14	60	12.04	Yixin Zhao and Zhu (2014)
2.	ITO/MoO_3/PEDOT:PSS/PSK/C_{60} B-phen/Ag	Planar p-i-n	Spin coating	–		0.96	20.06	67	12.78	Hou et al. (2015)
3.	ITO/MoO_3/NPB/PSK/C_{60}/BCP/Al	Planar p-i-n	Thermal evaporation	5 nm		1.12	18.1	68	13.7	Kim et al. (2015)
4.	FTO/TiO_2/PSK/spiro/MoO_x/Ag	Planar n-i-p	Spin coating	50 nm		0.938	18.5	0.67	11.6	Sanehira et al. (2016)
5.	ITO/PEDOT: PSS/$CH_3NH_3PbIxCl_{3-x}$/PC61BM/-Bphen/Ag	Planar p-i-n	Spin coating	5 nm	350–800	0.71	16.93	0.61	7.46	Lou and Wang (2017)
6.	ITO/PEDOT: PSS- MoO_3/$CH_3NH_3PbIxCl_{3-x}$/PC61BM/B-phen/Ag					0.70	17.01	0.63	7.58	
7.	ITO/PEDOT: PSS-GeO_2/$CH_3NH_3PbIxCl_{3-x}$/PC61BM/ Bphen/Ag					0.72	17.26	0.63	7.83	
8.	ITO/PEDOT: PSS-V_2O_5/$CH_3NH_3PbIxCl_{3-x}$/PC61BM/ Bphen/Ag					0.73	17.35	0.66	8.36	
9.	ITO/PEDOT: PSS-CrO_3/$CH_3NH_3PbIxCl_{3-x}$/PC61BM/ Bphen/Ag					0.68	15.63	0.60	6.38	

Zhang et al. (2016) used low-temperature-processed (100 °C) carbon paste in PSCs and reported an impressive PCE value of 8.31% and here carbon acts as both counter electrode and as hole transporter. Impedance spectroscopy results show that good charge transport characteristics are exhibited by a low-temperature processed carbon material. Moreover, long-term stability studies show that the carbon-based PSCs exhibit good stability even after 800 h. Further, the crystallite size and morphology of carbon materials play a key role in determining the performance of the cell as they influence the electrical contact at the $CH_3NH_3PbI_3$/Carbon interface (Yang et al., 2014). They have reported that PSCs with carbon made of smallest graphite flakes and carbon black particles exhibit the highest efficiency of 10.2%. The performance of carbon PSCs shows that it is possible soon to develop low-cost and highly efficient flexible PSCs. Moreover, they have suggested that the material contact between carbon and perovskite layer is the key to achieve good performance in PSCs. Wei et al. (2014) have reported that candle soot is an effective hole extractor and is a cost-effective, environmentally stable and abundantly available material. They have developed PSCs by interfacing the candle soot with $CH_3NH_3PbI_3$ films. The fabricated solar cells exhibited a remarkable efficiency of 11.02% and good long-term stability. Femtosecond time-resolved PL and distance-dependent PL measurements have confirmed that the improved PCE is largely due to the enhanced directional hole extraction. They have also fabricated planar carbon-based PSCs that have a nano-carbon hole-extraction layer prepared by inkjet printing technique with a precisely controlled pattern and low interface. This inkjet printing technique could not only be used to precisely control the pattern of the carbon electrode, but also improve the interface between the $CH_3NH_3PbI_3$ active layer and the carbon hole-extraction electrode. As a result, considerably higher power conversion efficiency of 11.60% has been achieved. Liu et al. (2015) have fabricated carbon-based PSCs devices by effectively depositing uniform and continuous $MAPbI_3$ onto ZrO_2/TiO_2 films by a sequential deposition method and obtained a high efficiency of 13.14%. They have concluded that some of the parameters, like the thickness of spacer layer, pore filling and morphology of $CH_3NH_3PbI_3$ perovskite, the temperature of substrate and precursor greatly influence the performance of these types of solar cells.

Zhang et al. (2015) have reported about the effect of the size of the graphite layer on the performance of the cell and they have stated that an overly thick layer of carbon counter electrode (CCE) will restrict the diffusion of the PbI_2 precursor from the CCE layer to the TiO_2 layer, resulting in incomplete pore filling. Therefore, the thickness of the CCEs should be optimized. They have fabricated devices using graphite-based carbon materials of different thicknesses (40 nm, 500 nm, 3 μm, 6 μm, 8 μm), among these, the device with 8 μm graphite thickness had a larger average pore size, smaller square resistance and hence a higher PCE exceeding 11%. It confirms that graphite thickness has a huge influence on the porosity and conductivity of carbon. Wei et al. (2015) have synthesized free-standing thermoplastic carbon film with good flexibility and conductivity and introduced it in PSCs. Due to its unique nature of thermo-plasticity, this free-standing carbon film can be directly hot pressed onto the perovskite layer as a counter electrode. By optimizing the weight ratio between graphite and carbon black to 3:1 an increase in J_{SC} from 18.77 to

Table 8 Photovoltaic characteristics of perovskite solar cells using carbon as a hole-transport-free layer.

S. no.	Device gestalt	Structure type	Hole-transport-free layer		IPCE (response range) (nm)	Photovoltaic parameters				Ref.
			Method	Thickness		V_{OC} (V)	J_{SC} (mA/cm^2)	FF (%)	η (%)	
1.	FTO/TiO_2/PSK/C (candle soot)	Mesoporous n-i-p	Doctor blade	10 μm	–	0.88	16.50	67	11.02	Wei et al. (2014)
2.	FTO/TiO_2/PSK/ZrO_2/C	Mesoporous n-i-p	Hot press	10 μm	300–800	0.90	17.42	66	10.30	Liu et al. (2015)
3.	FTO/TiO_2/Mixed cation -PSK + ZrO_2/C	Multilayered n-i-p	Screen print	1–2 μm	350–800	0.85	22.8	66	12.84	Zhang et al. (2015)
4.	FTO/TiO_2/PSK/C/Al	Mesoporous n-i-p	Hot press	40 μm	–	1	21.02	63	13.53	Wei et al. (2015)
5.	FTO/TiO_2/PSK/C + Graphite	Mesoporous n-i-p	Screen print	23 μm	–	0.952	18.73	57	10.20	Yang et al. (2014)
6.	FTO/c-TiO_2/m-TiO_2/PSK/C	Mesoporous n-i-p	Doctor blade	20 μm	400–800	0.75	17.30	53	6.90	Zhou et al. (2014)
7.	FTO/TiO_2/PSK/C	Planar n-i-p	Inkjet print	–	550–800	0.95	17.20	71	11.60	Wei et al. (2014)
8.	FTO/TiO_2/PSK/C	Planar n-i-p	Spin coating	10–50 μm	–	1.01	14.20	60	8.61	Chen et al. (2014)
9.	FTO/ZnO/PSK/C	Planar n-i-p	Doctor blade	–	400–800	0.77	18.16	51	7.26	Zhou et al. (2014)
10.	FTO/TiO_2/PSK/C	Planar n-i-p	Doctor blade	15 μm	400–800	0.87	16.10	52.6	7.40	Zhang et al. (2016)
11.	FTO/TiO_2/ZrO_2/PSK/C	Planar n-i-p	Screen print	9 μm	400–800	0.84	18.06	72	11.63	Zhang et al. (2015)

Table 9 Photovoltaic characteristics of perovskite solar cells using graphene oxide/reduced graphene oxide as HTMs.

S. no.	Device gestalt	Structure type	Graphene oxide/reduced graphene oxide hole transporting layer		IPCE (response range) (nm)	Photovoltaic parameters				Ref.
			Method	Thickness		V_{OC} (V)	J_{SC} (mA/cm^2)	FF (%)	η (%)	
1.	FTO/PSK/GO	Planar n-i-p	Spin coating	150 nm	–	1.03	20.20	73	15.1	Li et al. (2014)
2.	ITO/GO/PEDOT: PSS/PSK/PCBM/Al	n-i-p	Doctor blade	–	400–800	0.96	17.96	76	13.1	Li et al. (2016)
3.	ITO/r-GO/PSK/PCBM/BCP/Al	n-i-p	–	3 nm	300–800	0.95	14.81	71.13	9.95	Yeo et al. (2015)
4.	FTO/TiO_2/PSK/r-GO/Au	Planar n-i-p	Spray	–	300–800	0.95	11.50	60.5	6.62	Palma et al. (2016)

Please cite this article in press as: Pitchaiya, S. et al., A review on the classification of organic/inorganic/carbonaceous hole transporting materials for perovskite solar cell application. Arabian Journal of Chemistry (2018), https://doi.org/10.1016/j.arabjc.2018.06.006

21.30 mA/cm^2 was achieved and the FF improved from 0.566 to 0.634, yielding the highest PCE of 13.53%, which is one of the highest efficiencies reported for PSCs fabricated without an HTL.

The device structures, thickness of the HTMs used, the IPCE and photovoltaic parameters of the PSCs fabricated using carbon are given in the Tables 8 and 9 (as a hole-transport-free layer in Table 8 & as HTL in Table 9). Fig. 13 provides an energy-level alignment diagram of the device components of PSCs in which (relative to vacuum level) a carbon-based hole-transport-free layer (p-i-n) is shown.

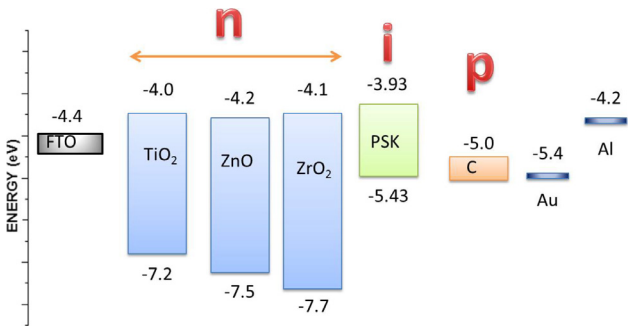

Fig. 13 Energy-level alignment diagram of the device components of perovskite solar cells with (relative to vacuum level) carbon as hole-transport-free material (n-i-p).

6.2. Graphene and doped graphene oxide based HTMs

Compared to carbon materials, graphene oxide (GO) and reduced graphene oxides (r-GO), which have a two-dimensional sheet structure consisting of carbon atom monolayer, are considered to have a great potential to be used in PSCs as they exhibit good electrical conductivity and high specific surface area (Cho et al., 2014). The high electrical conductivity is due to the extremely high electron mobility and fast heterogeneous electron transfer (Jaison et al., 2015). Therefore, due to the afore-mentioned properties, graphene derivatives GO and r-GO have been used as a substitute for spiro-OMeTAD as HTM in PSCs. This could be a viable strategy both economically and technically, i.e., due to mobility values and stability of the device (Liu et al., 2015; Yeo et al., 2015). Replacing the organic HTL by GO may result in better efficiency and then for improving the cell stability, r-GO could be a good choice.

During the initial stages when GO was introduced as HTM in PSCs, it was employed just as a bilayer along with PEDOT: PSS. This GO bilayer modification strategy takes the advantages of the high conductivity of PEDOT: PSS and good electron-blocking capability of GO, and produces a marked increase in PCE from 10% to 13.1%.

Li et al. (2014) have studied the interface properties of PSCs and reported that the interface wettability of the HTL solution on a perovskite surface could be improved. To address this problem, GO with amphiphilic function is used to form a buffer layer between the perovskite and the HTL. After the GO modification, the contact angle of the HTL solution with the perovskite film decreased to zero degrees. The GO layer improved the contact between the perovskite and HTL, resulting in an enhancement of the short-circuit current density. Moreover, using GO as an insulating buffer layer can retard charge recombination in solar cells, as revealed by EIS measured in dark conditions, leading to a significant increase in the open-circuit voltage and the fill factor. Therefore, application of GO as a dual-function buffer layer on the perovskite layer is a useful strategy for preparing highly efficient hybrid PSCs. Yeo et al. (2015) are the first research group to introduce r-GO, as a novel HTM and fabricate and highly efficient and stable $CH_3NH_3PbI_3$ PSCs. The fabricated device exhibited excellent and reproducible device efficiency up to 10.8%, which was superior to the PEDOT: PSS and GO-based devices. A systematic investigation on the mechanisms responsible for the efficiency enhancement of r-GO devices revealed that the facilitated charge collection with a retarded recombination, high r-GO conductivity, better-aligned energy levels, and better growth of the perovskites on r-GO HTMs are responsible for the high efficiency. More importantly, in the ambient stability test, they found that the use of r-GO HTMs with the inherent passivation-ability greatly extended the cell lifetime compared to PSCs employing conventional PEDOT: PSS. These successful demonstrations showed r-GO to be an advanced interfacial material which has the potential to replace the conventional PEDOT: PSS HTMs because of the observed photovoltaic performance and device-stability.

Palma et al. (2016) have demonstrated the application of reduced graphene oxide as effective HTM for the long-term stability of PSCs. They have reported about the stability study that a 1987 h' shelf life test showed that r-GO-based PSCs shows 36% increase of efficiency (PCE = 6.6%), with respect to the value recorded by r-GO-based PSCs (PCE = 4.87%). The results of endurance tests showed that the reduced graphene oxide is not affected by the issues of additives as tBP which corrodes the perovskite material when used as an additive in spiro-OMeTAD. The increase of the PCE in the r-GO-based PSCs can be related to the reduction in the density of charged bulk defects within the perovskite layer due to the light illumination during measurements.

The device structure, and thickness of the HTMs used, IPCE and photovoltaic parameters of the PSCs fabricated using carbonaceous materials GO and r-GO as HTMs are given in Table 9. Fig. 14 shows the energy-level alignment diagram of the device components of PSCs in which (relative to

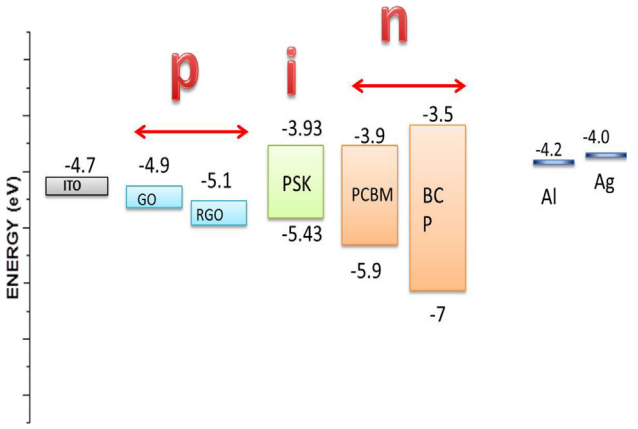

Fig. 14 Energy-level alignment diagram of the device components of perovskite solar cells with (relative to vacuum level) graphene oxide/reduced graphene oxide as HTMs in (p-i-n).

Table 10 Stability and Photovoltaic behavior of perovskite solar cells with different class of HTMs.

Class of HTMS	Device gestalt	Achieved efficiency (η)				Efficiency after aging (η)	Stability duration (in hours)	Ambient condition (RT means room temperature)	Ref.
		J_{SC} (mA/cm^2)	V_{OC} (V)	FF (%)	η (%)				
Nickel based HTMs	FTO/TiO_2/Al_2O_3/NiO/SWCNT/($MAPbI_3$)	20.70	0.95	64	12.7	12.46	300	40–60%, humidity, 25C in dark	Liu et al. (2017)
	FTO/TiO_2/Al_2O_3/NiO/carbon black/($MAPbI_3$)/graphite	18.86	0.93	58	10.50	10.23	300	40–60%, humidity, 25 °C in dark	
	FTO/NiO/$MAPbI_3$/PCBM/Ag	20.7	0.99	77	15.71	15.10	1500	30% humidity in RT.	Yin et al. (2017)
Copper based HTMs	FTO/TiO_2/$MAPbI_3$/CuPc-OTPABu/Carbon	21.9	1.00	68	15.00	10	720	30% humidity in dark	Jiang et al. (2017)
	FTO/TiO_2/$MAPbI_3$/Cu-NiO_2/Ag	21.58	1.11	81	19.62	15.6	1000	35% humidity, 25 °C in dark	Yao et al. (2017)
Polymer-based HTMs	FTO/TiO_2/MAPbI3/spiro-OMeTAD/Au	20	1.00	70	15.00	12	480	50–70%, humidity, 20–30 °C in dark	Ren et al. (2017)
	FTO/TiO_2/MAPbI3/spiro-OMeTAD/Au	23.4	1.15	77	20.8	19.3	480	20% humidity at RT	Xu et al. (2017)
	FTO/TiO_2/MAPbI3/spiro-OMeTAD/Au	19.17	1.16	70	13.65	3.9	600	30% humidity at RT	Sun et al. (2017)
	FTO/TiO_2/MAPbI3/spiro-OMeTAD/Au	15.7	1.02	68.8	11.06	4.9	138	30% humidity at RT	Palma et al. (2016)
	ITO/PC_{61}BM/$MAPbI_3$/CNO: PEDOT: PSS/Ag	17.28	0.90	71	11.07	0	120	40% humidity at RT in dark	Zheng et al. (2017)
	ITO/PEDOT: PSS/$MAPbI_3$/PC_{71}BM/Ca/Al	23.51	1.03	0.83	20.1	1.7	120	40% humidity at 25 °C	Chiang et al. (2017)
	FTO/PC_{61}BM/$MAPbI_3$/PEDOT: PSS/Au	16.26	0.73	64	7.63	2.4	72	35% humidity at RT in dark	Reddy et al. (2016)
	FTO/TiO_2/$MAPbI_3$/P3HT-F4TCNQ/Au	19.5	0.96	55	14.4	11.9	960	30% humidity, RT in dark	Zhang et al. (2016)
	FTO/TiO_2/$MAPbI_3$/P3HT-GD/Au	19.63	0.94	71	13.17	11.8	2520	30% humidity, RT in dark	Xiao et al. (2015)
	FTO/TiO_2/$MAPbI_3$/P3HT/Au	17.51	0.95	61	11.11	9.9	2520	30% humidity, RT in dark	
Carbonaceous based HTMs	ITO/PC_{61}BM/$MAPbI_3$/CNO: PEDOT: PSS/Ag	21.34	0.94	76	15.26	11.2	240	40% humidity, RT in dark	Zheng et al. (2017)
	ITO/PC_{61}BM/$MAPbI_3$/CNO: PEDOT: PSS/Ag	20.99	0.92	72.5	14.04	9.3	240	40% humidity, RT in dark	
	ITO/PC_{61}BM/$MAPbI_3$/r-GO/Ag	8.95	0.91	59.7	4.87	3.8	2000	40% humidity, RT in dark	Palma et al. (2016)
Organic Small molecule based HTMs	ITO/PC_{61}BM/$MAPbI_3$/ATT-OMe/Al	21.75	1.07	78	18.13	11.8	400	30% humidity, RT in dark	Zimmermann et al. (2017)
	ITO/PC_{61}BM/$MAPbI_3$/ATT-OHe_x/Ag	19.60	1.03	78	15.66	8.4	400	30% humidity, RT in dark	
	ITO/PC_{61}BM/$MAPbI_3$/ATT-OBu/Ag	20.94	1.05	78	17.28	9.5	300	30% humidity, RT in dark	
	ITO/PC_{61}BM/$MAPbI_3$/CzPAF-SBF/Al	16.31	0.74	65	7.85	4.1	180	40% humidity, RT in dark	Reddy et al. (2016)
	ITO/PC_{61}BM/$MAPbI_3$/CzPAF-SBFN/Au	15.43	0.73	58	6.50	2.8	200	40% humidity, RT in dark	

Please cite this article in press as: Pitchaiya, S. et al., A review on the classification of organic/inorganic/carbonaceous hole transporting materials for perovskite solar cell application. Arabian Journal of Chemistry (2018), https://doi.org/10.1016/j.arabjc.2018.06.006

vacuum level) carbonaceous materials GO and r-GO are used as HTMs (p-i-n).

7. Stability chart for various HTMs in PSCs

Although PSCs have shown incomparable photovoltaic performance in almost all their device architectures using various kinds of organic/inorganic/carbonaceous based HTMs, they are known to degrade when exposed to atmospheric conditions such as humidity, temperature, light, air, and water. The predominant reasons for instability are its intrinsic structural instability that arises from the fact that the materials constituting a perovskite crystal are chemically unstable. Based on the stability crisis of PSCs, we have studied the recent reports of the different kind of HTMs used and have provided a summary of its device structure (ETL and HTL used), its photovoltaic parameters (V_{OC}, J_{SC}, FF and efficiency (η)), reliable in its efficiency after aging and stability duration under ambient conditions which will undoubtedly provide overall knowledge on the selection of HTMs for PSCs with improved efficiency and with improved stability (shown in Table 10).

From this stability chart, we could infer that the stability of perovskite devices depend on the HTMs we use. Nickel-based HTM resulted in achieving efficiency of 15.71% and remains stable for nearly 1500 h under 30% humidity at RT. Whereas copper based HTM resulted in achieving higher efficiency (19.62%) than that of the nickel-based HTMs but failed to retain its stability after aging (1000 h under 35% humidity, 25 °C in dark). Further, polymer-based HTMs (spiro-OMeTAD) though resulted in achieving 20.1% of PCE exhibited poor stability (about 480 h) even under 20% humidity at RT. Similarly, organic small molecules based HTMs though resulted in achieving higher PCE but could retain only for about 400 h. On the other hand, HTMs based on carbon resulted in achieving the long-term stability of about 2500 h but have achieved only 11.11% PCE. Organic polymer HTM based perovskite solar cells having an efficiency >20% provides much hope for a high performance; however, few unsolved issues such as its structure and cost prevents them from pratical adaptability and most important of which is its challenging operational stability. To develop a stable device, one should understand the origin of its instability, which in turn requires a clear understanding of the structural and morphological properties of the hole transporting material we use in the device. Though we have a wide variety of available device architecture for achieving both stability and performance, PSCs also have environmental and economic drawbacks which are to be overcome.

8. Conclusion outlook

In this present review, a thorough study has been made about the significant progress which have taken place in the organic, inorganic and carbonaceous based HTMs used in PSCs. The overview provides details about the two important aspects i.e. efficiency and stability. Organic HTMs are found to be advantageous in terms of efficiency, however, it fails in ensuring long-term stability, while inorganic HTMs are found to be better when considering stability factor, but shows poor efficiency. In addition to these properties of various carbon-based materials used in PSCs have been discussed, which are found to be better candidates in terms of device performance and stability. The latest development of HTM free carbon-based materials used in PSCs has also been discussed.

In summary, this article is about the critical challenges involved in the synthesis and device engineering of various types of HTMs used in PSC devices and may help to identify some key issues which are to be addressed to further enhance the performanceand improve the stability of PSC devices. The future research is all about inexpensive, non-toxic and environmental friendly materials suitable for the different components of PSC exhibiting better performance with improved device stability.

Acknowledgment

Authors gratefully acknowledge the financial support provided by TEQIP - Coimbatore Institute of Technology, Coimbatore, India and Western Norway University of Applied Sciences, UTFORSK program, Bergen, Norway.

Notes

The authors declare no competing financial interest.

References

Abdulrazzaq, O.A., Saini, V., Bourdo, S., Dervishi, E., Biris, A.S., 2013. Organic solar cells: A review of materials, limitations, and possibilities for improvement. Part. Sci. Technol. 31, 427–442.

Ahirrao, P., Gosavi, S., Sonawane, S.S., Patil, R., 2011. Wide band gap nanocrystalline CuSCN thin films deposited by modified chemical method. Arch. Phys. Res. 2, 29–33.

Aitola, K., Sveinbjornsson, K., Correa-Baena, J.-P., Kaskela, A., Abate, A., Tian, Y., Johansson, E.M.J., Gratzel, M., Kauppinen, E.I., Hagfeldt, A., Boschloo, G., 2016. Carbon nanotube-based hybrid hole-transporting material and selective contact for high efficiency perovskite solar cells. Energy Environ. Sci. 9, 461–466.

Ameen, S., Rub, M.A., Kosa, S.A., Alamry, K.A., Akhtar, M.S., Shin, H.-S., Seo, H.-K., Asiri, A.M., Nazeeruddin, M.K., 2016. Perovskite solar cells: influence of hole transporting materials on power conversion efficiency. ChemSusChem 9, 10–27.

Bach, U., Lupo, D., Comte, P., Moser, J., Weissörtel, F., Salbeck, J., Spreitzer, H., Grätzel, M., 1998. Solid-state dye-sensitized mesoporous TiO 2 solar cells with high photon-to-electron conversion efficiencies. Nature 395, 583.

Bakr, Z.H., Wali, Q., Fakharuddin, A., Schmidt-Mende, L., Brown, T.M., Jose, R., 2017. Advances in hole transport materials engineering for stable and efficient perovskite solar cells. Nano Energy 34, 271–305.

Ball, J.M., Lee, M.M., Hey, A., Snaith, H.J., 2013. Low-temperature processed meso-superstructured to thin-film perovskite solar cells. Energy Environ. Sci. 6, 1739–1743.

Batmunkh, Munkhbayar, Shearer, Cameron J., Biggs, M.J., Shapter, J.G., 2015. Nanocarbons for mesoscopic perovskite solar cells. J. Mater. Chem. A.

Burschka, J., Pellet, N., Moon, S.-J., Humphry-Baker, R., Gao, P., Nazeeruddin, M.K., Grätzel, M., 2013. Sequential deposition as a route to high-performance perovskite-sensitized solar cells. Nature 499, 316.

Cai, B., Xing, Y., Yang, Z., Zhang, W.-H., Qiu, J., 2013. High performance hybrid solar cells sensitized by organolead halide perovskites. Energy Environ. Sci. 6, 1480–1485.

Calió, L., Kazim, S., Grätzel, M., Ahmad, S., 2016. Hole-transport materials for perovskite solar cells. Angew. Chem. Int. Ed. 55, 14522–14545.

Cao, K., Zuo, Z., Cui, J., Shen, Y., Moehl, T., Zakeeruddin, S.M., Grätzel, M., Wang, M., 2015. Efficient screen printed perovskite solar cells based on mesoscopic TiO2/Al2O3/NiO/carbon architecture. Nano Energy 17, 171–179.

Chavhan, S., Miguel, O., Grande, H.-J., Gonzalez-Pedro, V., Sanchez, R.S., Barea, E.M., Mora-Sero, I., Tena-Zaera, R., 2014. Organo-metal halide perovskite-based solar cells with CuSCN as the inorganic hole selective contact. J. Mater. Chem. A 2, 12754–12760.

Chen, W.-Y., Deng, L.-L., Dai, S.-M., Wang, X., Tian, C.-B., Zhan, X.-X., Xie, S.-Y., Huang, R.-B., Zheng, L.-S., 2015. Low-cost solution-processed copper iodide as an alternative to PEDOT:PSS hole transport layer for efficient and stable inverted planar heterojunction perovskite solar cells. J. Mater. Chem. A 3, 19353–19359.

Chen, Z., Li, H., Zheng, X., Zhang, Q., Li, Z., Hao, Y., Fang, G., 2017. Low-cost carbazole-based hole transport material for highly efficient perovskite solar cells. ChemSusChem.

Chen, S., Liu, P., Hua, Y., Li, Y., Kloo, L., Wang, X., Ong, B., Wong, W.-K., Zhu, X., 2017. Study of arylamine-substituted porphyrins as hole-transporting materials in high-performance perovskite solar cells. ACS Appl. Mater. Interfaces 9, 13231–13239.

Chen, H., Pan, X., Liu, W., Cai, M., Kou, D., Huo, Z., Fang, X., Dai, S., 2013. Efficient panchromatic inorganic-organic heterojunction solar cells with consecutive charge transport tunnels in hole transport material. Chem. Commun. 49, 7277–7279.

Chen, D., Wang, Y., Lin, Z., Huang, J., Chen, X., Pan, D., Huang, F., 2010. Growth strategy and physical properties of the high mobility P-type CuI crystal. Cryst. Growth Des. 10, 2057–2060.

Chen, H., Wei, Z., Yan, K., Yi, Y., Wang, J., Yang, S., 2014. Liquid phase deposition of TiO2 nanolayer affords CH3NH3PbI3/nanocarbon solar cells with high open-circuit voltage. Faraday Discuss. 176, 271–286.

Chen, B., Yang, M., Priya, S., Zhu, K., 2016. Origin of J-V hysteresis in perovskite solar cells. J. Phys. Chem. Lett. 7, 905–917.

Chen, H., Yang, S., 2017. Carbon-based perovskite solar cells without hole transport materials: the front runner to the market? Adv. Mater. 29. 1603994-n/a.

Chia-Ching, W., Cheng-Fu, Y., 2013. Investigation of the properties of nanostructured Li-doped NiO films using the modified spray pyrolysis method. Nanoscale Res. Lett. 8, 33.

Chiang, C.-H., Nazeeruddin, M.K., Gratzel, M., Wu, C.-G., 2017. The synergistic effect of H2O and DMF towards stable and 20% efficiency inverted perovskite solar cells. Energy Environ. Sci. 10, 808–817.

Cho, K.T., Lee, S.B., Lee, J.W., 2014. Facile synthesis of highly electrocapacitive nitrogen-doped graphitic porous carbons. J. Phys. Chem. C 118, 9357–9367.

Chou, H.-H., Chiang, Y.-H., Li, M.-H., Shen, P.-S., Wei, H.-J., Mai, C.-L., Chen, P., Yeh, C.-Y., 2016. Zinc porphyrin-ethynylaniline conjugates as novel hole-transporting materials for perovskite solar cells with power conversion efficiency of 16.6%. ACS Energy Lett. 1, 956–962.

Christians, J.A., Fung, R.C.M., Kamat, P.V., 2014. An inorganic hole conductor for organo-lead halide perovskite solar cells. Improved hole conductivity with copper iodide. J. Am. Chem. Soc. 136, 758–764.

Cong, H., Han, D., Sun, B., Zhou, D., Wang, C., Liu, P., Feng, L., 2017. Facile approach to preparing a vanadium oxide hydrate layer as a hole-transport layer for high-performance polymer solar cells. ACS Appl. Mater. Interfaces 9, 18087–18094.

Correa-Baena, J.-P., Abate, A., Saliba, M., Tress, W., Jesper Jacobsson, T., Gratzel, M., Hagfeldt, A., 2017. The rapid evolution of highly efficient perovskite solar cells. Energy Environ. Sci. 10, 710–727.

Cui, J., Meng, F., Zhang, H., Cao, K., Yuan, H., Cheng, Y., Huang, F., Wang, M., 2014. CH3NH3PbI3-based planar solar cells with magnetron-sputtered nickel oxide. ACS Appl. Mater. Interfaces 6, 22862–22870.

Daskeviciene, M., Paek, S., Wang, Z., Malinauskas, T., Jokubauskaite, G., Rakstys, K., Cho, K.T., Magomedov, A., Jankauskas, V., Ahmad, S., Snaith, H.J., Getautis, V., Nazeeruddin, M.K., 2017. Carbazole-based enamine: Low-cost and efficient hole transporting material for perovskite solar cells. Nano Energy 32, 551–557.

Dhakal, R., Huh, Y., Galipeau, D., Yan, X., 2011. AlSb compound semiconductor as absorber layer in thin film solar cells, in: Solar Cells-New Aspects and Solutions. InTech.

Dhingra, P., Singh, P., Rana, P.J.S., Garg, A., Kar, P., 2016. Hole-transporting materials for perovskite-sensitized solar cells. Energy Technol. 4, 891–938.

Di Giacomo, F., Razza, S., Matteocci, F., D'Epifanio, A., Licoccia, S., Brown, T.M., Di Carlo, A., 2014. High efficiency CH3NH3PbI(3–x)Clx perovskite solar cells with poly(3-hexylthiophene) hole transport layer. J. Power Sources 251, 152–156.

Fakharuddin, A., De Rossi, F., Watson, T.M., Schmidt-Mende, L., Jose, R., 2016. Research update: Behind the high efficiency of hybrid perovskite solar cells. APL Mater. 4, 091505.

Fakharuddin, A., Schmidt-Mende, L., Garcia-Belmonte, G., Jose, R., Mora-Sero, I., 2017. Interfaces in perovskite solar cells. Adv. Energy Mater. 7, 1700623.

Galatopoulos, F., Savva, A., Papadas, I.T., Choulis, S.A., 2017. The effect of hole transporting layer in charge accumulation properties of p-i-n perovskite solar cells. APL Mater. 5. 076102.

Garcia, A., Welch, G.C., Ratcliff, E.L., Ginley, D.S., Bazan, G.C., Olson, D.C., 2012. Improvement of interfacial contacts for new small-molecule bulk-heterojunction organic photovoltaics. Adv. Mater. 24, 5368–5373.

Giorgi, G., Fujisawa, J.-I., Segawa, H., Yamashita, K., 2013. Small photocarrier effective masses featuring ambipolar transport in methylammonium lead iodide perovskite: a density functional analysis. J. Phys. Chem. Lett. 4, 4213–4216.

Gratia, P., Magomedov, A., Malinauskas, T., Daskeviciene, M., Abate, A., Ahmad, S., Gratzel, M., Getautis, V., Nazeeruddin, M. K., 2015. A Methoxydiphenylamine-substituted carbazole twin derivative: an efficient hole-transporting material for perovskite solar cells. Angew. Chem. Int. Ed. Engl. 54, 11409–11413.

Green, M.A., Emery, K., 1993. Solar cell efficiency tables. Prog. Photovoltaics Res. Appl. 1, 25–29.

Habisreutinger, S.N., Leijtens, T., Eperon, G.E., Stranks, S.D., Nicholas, R.J., Snaith, H.J., 2014. Carbon nanotube/polymer composites as a highly stable hole collection layer in perovskite solar cells. Nano Lett. 14, 5561–5568.

Habisreutinger, S.N., Wenger, B., Snaith, H.J., Nicholas, R.J., 2017. Dopant-free planar n–i–p perovskite solar cells with steady-state efficiencies exceeding 18%. ACS Energy Lett. 2, 622–628.

Hawash, Z., Ono, L.K., Raga, S.R., Lee, M.V., Qi, Y., 2015. Air-exposure induced dopant redistribution and energy level shifts in spin-coated spiro-MeOTAD films. Chem. Mater. 27, 562–569.

Hawash, Z., Ono, L.K., Qi, Y., 2018. Recent advances in spiro-MeOTAD hole transport material and its applications in organic-inorganic halide perovskite solar cells. Adv. Mater. Interfaces 5, 1700623.

Heo, J.H., Im, S.H., Noh, J.H., Mandal, T.N., Lim, C.-S., Chang, J. A., Lee, Y.H., Kim, H.-J., Sarkar, A., Nazeeruddin, M.K., Grätzel, M., Seok, S.I., 2013. Efficient inorganic–organic hybrid heterojunction solar cells containing perovskite compound and polymeric hole conductors. Nat. Photonics 7, 486.

Hideki, M., Asako, F., Tomohiro, K., 1996. Properties of high-mobility C u 2 O films prepared by thermal oxidation of Cu at low temperatures. Jpn. J. Appl. Phys. 35, 5631.

Hodes, G., 2013. Perovskite-based solar cells. Science 342, 317.

Hossain, M.I., Alharbi, F.H., Tabet, N., 2015. Copper oxide as inorganic hole transport material for lead halide perovskite based solar cells. Sol. Energy 120, 370–380.

Hou, F., Su, Z., Jin, F., Yan, X., Wang, L., Zhao, H., Zhu, J., Chu, B., Li, W., 2015. Efficient and stable planar heterojunction

perovskite solar cells with an MoO3/PEDOT:PSS hole transporting layer. Nanoscale 7, 9427–9432.
Hsiao, Y.-C., Wu, T., Li, M., Liu, Q., Qin, W., Hu, B., 2015. Fundamental physics behind high-efficiency organo-metal halide perovskite solar cells. J. Mater. Chem. A 3, 15372–15385.
Hu, X., Chen, L., Chen, Y., 2014. Universal and versatile MoO3-based hole transport layers for efficient and stable polymer solar cells. J. Phys. Chem. C 118, 9930–9938.
Hu, L., Peng, J., Wang, W., Xia, Z., Yuan, J., Lu, J., Huang, X., Ma, W., Song, H., Chen, W., Cheng, Y.-B., Tang, J., 2014. Sequential deposition of CH3NH3PbI3 on planar NiO film for efficient planar perovskite solar cells. ACS Photonics 1, 547–553.
Hua, Y., Zhang, J., Xu, B., Liu, P., Cheng, M., Kloo, L., Johansson, E.M.J., Sveinbjörnsson, K., Aitola, K., Boschloo, G., Sun, L., 2016. Facile synthesis of fluorene-based hole transport materials for highly efficient perovskite solar cells and solid-state dye-sensitized solar cells. Nano Energy 26, 108–113.
Huang, L., Hu, Z., Xu, J., Zhang, K., Zhang, J., Zhang, J., Zhu, Y., 2016. Efficient and stable planar perovskite solar cells with a non-hygroscopic small molecule oxidant doped hole transport layer. Electrochim. Acta 196, 328–336.
Huangfu, M., Shen, Y., Zhu, G., Xu, K., Cao, M., Gu, F., Wang, L., 2015. Copper iodide as inorganic hole conductor for perovskite solar cells with different thickness of mesoporous layer and hole transport layer. Appl. Surf. Sci. 357, 2234–2240.
Irwin, M.D., Buchholz, D.B., Hains, A.W., Chang, R.P.H., Marks, T.J., 2008. p-Type semiconducting nickel oxide as an efficiency-enhancing anode interfacial layer in polymer bulk-heterojunction solar cells. Proc. Natl. Acad. Sci. 105, 2783–2787.
Ito, S., Tanaka, S., Vahlman, H., Nishino, H., Manabe, K., Lund, P., 2014. Carbon-double-bond-free printed solar cells from TiO2/CH3NH3PbI3/CuSCN/Au: Structural control and photoaging effects. ChemPhysChem 15, 1194–1200.
Jaison, M.J., Narayanan, T.N., Prem Kumar, T., Pillai, V.K., 2015. A single-step room-temperature electrochemical synthesis of nitrogen-doped graphene nanoribbons from carbon nanotubes. J. Mater. Chem. A 3, 18222–18228.
Jeng, J.-Y., Chen, K.-C., Chiang, T.-Y., Lin, P.-Y., Tsai, T.-D., Chang, Y.-C., Guo, T.-F., Chen, P., Wen, T.-C., Hsu, Y.-J., 2014. Nickel oxide electrode interlayer in CH3NH3PbI3 perovskite/PCBM planar-heterojunction hybrid solar cells. Adv. Mater. 26, 4107–4113.
Jeon, N.J., Lee, J., Noh, J.H., Nazeeruddin, M.K., Grätzel, M., Seok, S.I., 2013. Efficient inorganic-organic hybrid perovskite solar cells based on pyrene arylamine derivatives as hole-transporting materials. J. Am. Chem. Soc. 135, 19087–19090.
Jiang, Y., Li, C., Liu, H., Qin, R., Ma, H., 2016. Poly(3,4-ethylenedioxythiophene):poly(styrenesulfonate)(PEDOT:PSS)-molybdenum oxide composite films as hole conductors for efficient planar perovskite solar cells. J. Mater. Chem. A 4, 9958–9966.
Jiang, X., Yu, Z., Zhang, Y., Lai, J., Li, J., Gurzadyan, G.G., Yang, X., Sun, L., 2017. High-performance regular perovskite solar cells employing low-cost poly(ethylenedioxythiophene) as a hole-transporting material. Sci. Rep. 7, 42564.
Jung, J.W., Chueh, C.-C., Jen, A.K.Y., 2015. High-performance semitransparent perovskite solar cells with 10% power conversion efficiency and 25% average visible transmittance based on transparent CuSCN as the hole-transporting material. Adv. Energy Mater. 5. 1500486-n/a.
Jung, M., Kim, Y.C., Jeon, N.J., Yang, W.S., Seo, J., Noh, J.H., Il, S., 2016. Seok, thermal stability of CuSCN hole conductor-based perovskite solar cells. ChemSusChem 9, 2592–2596.
Jung, J.W., Park, J.-S., Han, I.K., Lee, Y., Park, C., Kwon, W., Park, M., 2017. Flexible and highly efficient perovskite solar cells with a large active area incorporating cobalt-doped poly(3-hexylthiophene) for enhanced open-circuit voltage. J. Mater. Chem. A 5, 12158–12167.
Kang, M.S., Sung, S.D., Choi, I.T., Kim, H., Hong, M., Kim, J., Lee, W.I., Kim, H.K., 2015. Novel carbazole-based hole-transporting materials with star-shaped chemical structures for perovskite-sensitized solar cells. ACS Appl. Mater. Interfaces 7, 22213–22217.
Kim, H.-S., Jang, I.-H., Ahn, N., Choi, M., Guerrero, A., Bisquert, J., Park, N.-G., 2015. Control of I-V hysteresis in CH3NH3PbI3 perovskite solar cell. J. Phys. Chem. Lett. 6, 4633–4639.
Kim, B.-S., Kim, T.-M., Choi, M.-S., Shim, H.-S., Kim, J.-J., 2015. Fully vacuum–processed perovskite solar cells with high open circuit voltage using MoO3/NPB as hole extraction layers. Org. Electron. 17, 102–106.
Kim, J.H., Liang, P.-W., Williams, S.T., Cho, N., Chueh, C.-C., Glaz, M.S., Ginger, D.S., Jen, A.K.Y., 2015. High-performance and environmentally stable planar heterojunction perovskite solar cells based on a solution-processed copper-doped nickel oxide hole-transporting layer. Adv. Mater. 27, 695–701.
Kojima, A., Teshima, K., Shirai, Y., Miyasaka, T., 2009. Organometal halide perovskites as visible-light sensitizers for photovoltaic cells. J. Am. Chem. Soc. 131, 6050–6051.
Korzhavyi, P.A., Johansson, B., 2011. Literature review on the properties of cuprous oxide Cu2O and the process of copper oxidation. Swedish Nucl. Fuel Waste Manage. Company.
Krishna, A., Grimsdale, A.C., 2017. Hole transporting materials for mesoscopic perovskite solar cells - towards a rational design? J. Mater. Chem. A 5, 16446–16466.
Krishnamoorthy, T., Kunwu, F., Boix, P.P., Li, H., Koh, T.M., Leong, W.L., Powar, S., Grimsdale, A., Gratzel, M., Mathews, N., Mhaisalkar, S.G., 2014. A swivel-cruciform thiophene based hole-transporting material for efficient perovskite solar cells. J. Mater. Chem. A 2, 6305–6309.
Kumar, C.V., Sfyri, G., Raptis, D., Stathatos, E., Lianos, P., 2015. Perovskite solar cell with low cost Cu-phthalocyanine as hole transporting material. RSC Adv. 5, 3786–3791.
Kurnia, F., Hadiyawarman, H., Jung, C.U., Liu, C.L., Lee, S.B., Yang, S.M., Park, H.W., Song, S.J., Hwang, C.S., 2010. Effect of NiO growth conditions on the bipolar resistance memory switching of Pt/NiO/SRO structure. J. Korean Phys. Soc. 57, 1856–1861.
Lattante, S., 2014. Electron and hole transport layers: their use in inverted bulk heterojunction polymer solar cells. Electronics 3, 132–164.
Lee, U.-H., Azmi, R., Sinaga, S., Hwang, S., Eom, S.H., Kim, T.-W., Yoon, S.C., Jang, S.-Y., Jung, I.H., 2017. Diphenyl-2-pyridylamine-substituted porphyrins as hole-transporting materials for perovskite solar cells. ChemSusChem 10, 3780–3787.
Lee, M.M., Teuscher, J., Miyasaka, T., Murakami, T.N., Snaith, H. J., 2012. Efficient hybrid solar cells based on meso-superstructured organometal halide perovskites. Science 338, 643.
Li, D., Cui, J., Li, H., Huang, D., Wang, M., Shen, Y., 2016. Graphene oxide modified hole transport layer for CH3NH3PbI3 planar heterojunction solar cells. Sol. Energy 131, 176–182.
Li, W., Dong, H., Wang, L., Li, N., Guo, X., Li, J., Qiu, Y., 2014. Montmorillonite as bifunctional buffer layer material for hybrid perovskite solar cells with protection from corrosion and retarding recombination. J. Mater. Chem. A 2, 13587–13592.
Li, W., Dong, H., Guo, X., Li, N., Li, J., Niu, G., Wang, L., 2014. Graphene oxide as dual functional interface modifier for improving wettability and retarding recombination in hybrid perovskite solar cells. J. Mater. Chem. A 2, 20105–20111.
Li, H., Fu, K., Hagfeldt, A., Grätzel, M., Mhaisalkar, S.G., Grimsdale, A.C., 2014. A simple 3,4-ethylenedioxythiophene based hole-transporting material for perovskite solar cells. Angew. Chem. Int. Ed. 53, 4085–4088.
Li, M.-H., Shen, P.-S., Wang, K.-C., Guo, T.-F., Chen, P., 2015. Inorganic p-type contact materials for perovskite-based solar cells. J. Mater. Chem. A 3, 9011–9019.
Li, Z., Tinkham, J., Schulz, P., Yang, M., Kim, D.H., Berry, J., Sellinger, A., Zhu, K., 2017. Acid additives enhancing the conductivity of spiro-OMeTAD toward high-efficiency and hys-

Please cite this article in press as: Pitchaiya, S. et al., A review on the classification of organic/inorganic/carbonaceous hole transporting materials for perovskite solar cell application. Arabian Journal of Chemistry (2018), https://doi.org/10.1016/j.arabjc.2018.06.006

teresis-less planar perovskite solar cells. Adv. Energy Mater. 7, 1601451.
Li, M., Wang, Z.-K., Yang, Y.-G., Hu, Y., Feng, S.-L., Wang, J.-M., Gao, X.-Y., Liao, L.-S., 2016. Copper salts doped spiro-OMeTAD for high-performance perovskite solar cells. Adv. Energy Mater. 6, 1601156.
Li, M., Wang, Z.-K., Kang, T., Yang, Y., Gao, X., Hsu, C.-S., Li, Y., Liao, L.-S., 2018. Graphdiyne-modified cross-linkable fullerene as an efficient electron-transporting layer in organometal halide perovskite solar cells. Nano Energy 43, 47–54.
Li, Z.A., Zhu, Z., Chueh, C.-C., Luo, J., Jen, A.K.Y., 2016. Facile Thiol-Ene thermal crosslinking reaction facilitated hole-transporting layer for highly efficient and stable perovskite solar cells. Adv. Energy Mater. 6. 1601165.
Lin, Q., Jiang, W., Zhang, S., Nagiri, R.C.R., Jin, H., Burn, P.L., Meredith, P., 2017. A triarylamine-based anode modifier for efficient organohalide perovskite solar cells. ACS Appl. Mater. Interfaces 9, 9096–9101.
Liu, S., Cao, K., Li, H., Song, J., Han, J., Shen, Y., Wang, M., 2017. Full printable perovskite solar cells based on mesoscopic TiO2/Al2O3/NiO (carbon nanotubes) architecture. Sol. Energy 144, 158–165.
Liu, T., Liu, L., Hu, M., Yang, Y., Zhang, L., Mei, A., Han, H., 2015. Critical parameters in TiO2/ZrO2/Carbon-based mesoscopic perovskite solar cell. J. Power Sources 293, 533–538.
Liu, L., Xi, Q., Gao, G., Yang, W., Zhou, H., Zhao, Y., Wu, C., Wang, L., Xu, J., 2016. Cu2O particles mediated growth of perovskite for high efficient hole-transporting-layer free solar cells in ambient conditions. Sol. Energy Mater. Sol. Cells 157, 937–942.
Liu, D., Yongsheng, L., 2017. Recent progress of dopant-free organic hole-transporting materials in perovskite solar cells. J. Semicond. 38, 011005.
Liu, T., Yu, L., Liu, H., Hou, Q., Wang, C., He, H., Li, J., Wang, N., Wang, J., Guo, Z., 2017. Ni nanobelts induced enhancement of hole transport and collection for high efficiency and ambient stable mesoscopic perovskite solar cells. J. Mater. Chem. A 5, 4292–4299.
Liu, Z., Zhang, M., Xu, X., Bu, L., Zhang, W., Li, W., Zhao, Z., Wang, M., Cheng, Y.-B., He, H., 2015. p-Type mesoscopic NiO as an active interfacial layer for carbon counter electrode based perovskite solar cells. Dalton Trans. 44, 3967–3973.
Lou, Y.H., Wang, Z.K., 2017. Aqueous-solution-processable metal oxides for high-performance organic and perovskite solar cells. Nanoscale 9, 13506–13514.
Lu, C., Choi, I.T., Kim, J., Kim, H.K., 2017. Simple synthesis and molecular engineering of low-cost and star-shaped carbazole-based hole transporting materials for highly efficient perovskite solar cells. J. Mater. Chem. A 5, 20263–20276.
Luo, H., Lin, X., Hou, X., Pan, L., Huang, S., Chen, X., 2017. Efficient and air-stable planar perovskite solar cells formed on graphene-oxide-modified PEDOT:PSS hole transport layer. Nano-Micro Lett. 9, 39.
Madelung, O., 2004. Group VI elements. In: Madelung, O. (Ed.), Semiconductors: Data Handbook. Springer, Berlin Heidelberg, Berlin, Heidelberg, pp. 419–433.
Magomedov, A., Paek, S., Gratia, P., Kasparavicius, E., Daskeviciene, M., Kamarauskas, E., Gruodis, A., Jankauskas, V., Kantminiene, K., Cho, K.T., Rakstys, K., Malinauskas, T., Getautis, V., Nazeeruddin, M.K., 2018. Diphenylamine-substituted carbazole-based hole transporting materials for perovskite solar cells: influence of isomeric derivatives. Adv. Funct. Mater. 28, 1704351.
Mali, S.S., Hong, C.K., 2016. p-i-n/n-i-p type planar hybrid structure of highly efficient perovskite solar cells towards improved air stability: synthetic strategies and the role of p-type hole transport layer (HTL) and n-type electron transport layer (ETL) metal oxides. Nanoscale 8, 10528–10540.
Malinauskas, T., Saliba, M., Matsui, T., Daskeviciene, M., Urnikaite, S., Gratia, P., Send, R., Wonneberger, H., Bruder, I., Graetzel, M., Getautis, V., Nazeeruddin, M.K., 2016. Branched methoxydiphenylamine-substituted fluorene derivatives as hole transporting materials for high-performance perovskite solar cells. Energy Environ. Sci. 9, 1681–1686.
Matsui, T., Petrikyte, I., Malinauskas, T., Domanski, K., Daskeviciene, M., Steponaitis, M., Gratia, P., Tress, W., Correa-Baena, J.-P., Abate, A., Hagfeldt, A., Grätzel, M., Nazeeruddin, M.K., Getautis, V., Saliba, M., 2016. Additive-free transparent triarylamine-based polymeric hole-transport materials for stable perovskite solar cells. ChemSusChem 9, 2567–2571.
Momblona, C., Gil-Escrig, L., Bandiello, E., Hutter, E.M., Sessolo, M., Lederer, K., Blochwitz-Nimoth, J., Bolink, H.J., 2016. Efficient vacuum deposited p-i-n and n-i-p perovskite solar cells employing doped charge transport layers. Energy Environ. Sci. 9, 3456–3463.
Nguyen, W.H., Bailie, C.D., Unger, E.L., McGehee, M.D., 2014. Enhancing the hole-conductivity of spiro-OMeTAD without oxygen or lithium salts by using spiro(TFSI)2 in perovskite and dye-sensitized solar cells. J. Am. Chem. Soc. 136, 10996–11001.
Nia, N.Y., Matteocci, F., Cina, L., Di Carlo, A., 2017. High-efficiency perovskite solar cell based on poly(3-hexylthiophene): influence of molecular weight and mesoscopic scaffold layer. ChemSusChem 10, 3854–3860.
Noh, J.H., Im, S.H., Heo, J.H., Mandal, T.N., Seok, S.I., 2013. Chemical management for colorful, efficient, and stable inorganic-organic hybrid nanostructured solar cells. Nano Lett. 13, 1764–1769.
Ou, Q.D., Li, C., Wang, Q.K., Li, Y.Q., Tang, J.X., 2017. Recent advances in energetics of metal halide perovskite interfaces. Adv. Mater. Interfaces 4.
Palma, A.L., Cinà, L., Busby, Y., Marsella, A., Agresti, A., Pescetelli, S., Pireaux, J.-J., Di Carlo, A., 2016. Mesoscopic perovskite light-emitting diodes. ACS Appl. Mater. Interfaces 8, 26989–26997.
Park, I.J., Park, M.A., Kim, D.H., Park, G.D., Kim, B.J., Son, H.J., Ko, M.J., Lee, D.-K., Park, T., Shin, H., Park, N.-G., Jung, H.S., Kim, J.Y., 2015. New hybrid hole extraction layer of perovskite solar cells with a planar p–i–n geometry. J. Phys. Chem. C 119, 27285–27290.
Park, J.H., Seo, J., Park, S., Shin, S.S., Kim, Y.C., Jeon, N.J., Shin, H.-W., Ahn, T.K., Noh, J.H., Yoon, S.C., Hwang, C.S., Seok, S.I., 2015. Efficient CH3NH3PbI3 perovskite solar cells employing nanostructured p-type NiO electrode formed by a pulsed laser deposition. Adv. Mater. 27, 4013–4019.
Peng, H., Sun, W., Li, Y., Ye, S., Rao, H., Yan, W., Zhou, H., Bian, Z., Huang, C., 2016. Solution processed inorganic V2O x as interfacial function materials for inverted planar-heterojunction perovskite solar cells with enhanced efficiency. Nano Res. 9, 2960–2971.
Pitchaiya, S., Natarajan, M., Santhanam, A., Ramakrishnan, V.M., Asokan, V., Palanichamy, P., Rangasamy, B., Sundaram, S., Velauthapillai, D., 2018. Nickel sulphide-carbon composite hole transporting material for (CH 3 NH 3 PbI 3) planar heterojunction perovskite solar cell. Mater. Lett. 221, 283–288.
Prachumrak, N., Pojanasopa, S., Namuangruk, S., Kaewin, T., Jungsuttiwong, S., Sudyoadsuk, T., Promarak, V., 2013. Novel bis [5-(fluoren-2-yl) thiophen-2-yl] benzothiadiazole end-capped with carbazole dendrons as highly efficient solution-processed nondoped red emitters for organic light-emitting diodes. ACS Appl. Mater. Interfaces 5, 8694–8703.
Qian, M., Li, M., Shi, X.-B., Ma, H., Wang, Z.-K., Liao, L.-S., 2015. Planar perovskite solar cells with 15.75% power conversion efficiency by cathode and anode interfacial modification. J. Mater. Chem. A 3, 13533–13539.
Qin, P.-L., He, Q., Chen, C., Zheng, X.-L., Yang, G., Tao, H., Xiong, L.-B., Xiong, L., Li, G., Fang, G.-J., 2017. High-performance rigid and flexible perovskite solar cells with low-temperature solution-processable binary metal oxide hole-transporting materials. Solar RRL 1. 1700058-n/a.
Qin, P., Tanaka, S., Ito, S., Tetreault, N., Manabe, K., Nishino, H., Nazeeruddin, M.K., Grätzel, M., 2014. Inorganic hole conductor-

based lead halide perovskite solar cells with 12.4% conversion efficiency. Nat. Commun. 5, 3834.
Rajeswari, R., Mrinalini, M., Prasanthkumar, S., Giribabu, L., 2017. Emerging of inorganic hole transporting materials for perovskite solar cells. Chem. Rec. 17, 681–699.
Reddy, S.S., Gunasekar, K., Heo, J.H., Im, S.H., Kim, C.S., Kim, D.-H., Moon, J.H., Lee, J.Y., Song, M., Jin, S.-H., 2016. Highly efficient organic hole transporting materials for perovskite and organic solar cells with long-term stability. Adv. Mater. 28, 686–693.
Ren, Z., Zhu, M., Li, X., Dong, C., 2017. An isopropanol-assisted fabrication strategy of pinhole-free perovskite films in air for efficient and stable planar perovskite solar cells. J. Power Sources 363, 317–326.
Saliba, M., Orlandi, S., Matsui, T., Aghazada, S., Cavazzini, M., Correa-Baena, J.-P., Gao, P., Scopelliti, R., Mosconi, E., Dahmen, K.-H., De Angelis, F., Abate, A., Hagfeldt, A., Pozzi, G., Graetzel, M., Nazeeruddin, M.K., 2016. A molecularly engineered hole-transporting material for efficient perovskite solar cells. Nat. Energy 1, 15017.
Salim, T., Sun, S., Abe, Y., Krishna, A., Grimsdale, A.C., Lam, Y. M., 2015. Perovskite-based solar cells: impact of morphology and device architecture on device performance. J. Mater. Chem. A 3, 8943–8969.
Sanehira, E.M., Tremolet de Villers, B.J., Schulz, P., Reese, M.O., Ferrere, S., Zhu, K., Lin, L.Y., Berry, J.J., Luther, J.M., 2016. Influence of electrode interfaces on the stability of perovskite solar cells: reduced degradation using MoOx/Al for hole collection. ACS Energy Lett. 1, 38–45.
Sepalage, G.A., Meyer, S., Pascoe, A., Scully, A.D., Huang, F., Bach, U., Cheng, Y.-B., Spiccia, L., 2015. Copper(I) iodide as hole-conductor in planar perovskite solar cells: probing the origin of J-V hysteresis. Adv. Funct. Mater. 25, 5650–5661.
Song, Z., Watthage, S.C., Phillips, A.B., Heben, M.J., 2016. Pathways toward high-performance perovskite solar cells: review of recent advances in organo-metal halide perovskites for photovoltaic applications. J. Photonics Energy 6. 022001.
Subbiah, A.S., Halder, A., Ghosh, S., Mahuli, N., Hodes, G., Sarkar, S.K., 2014. Inorganic hole conducting layers for perovskite-based solar cells. J. Phys. Chem. Lett. 5, 1748–1753.
Sun, M., Liu, X., Zhang, F., Liu, H., Liu, X., Wang, S., Xiao, Y., Li, D., Meng, Q., Li, X., 2017. Simple dopant-free hole-transporting materials with p-π conjugated structure for stable perovskite solar cells. Appl. Surf. Sci. 416, 124–132.
Tang, C.W., 1986. Two-layer organic photovoltaic cell. Appl. Phys. Lett. 48, 183–185.
Teh, C.H., Daik, R., Lim, E.L., Yap, C.C., Ibrahim, M.A., Ludin, N. A., Sopian, K., Mat, M.A., 2016. Teridi, A review of organic small molecule-based hole-transporting materials for meso-structured organic–inorganic perovskite solar cells. J. Mater. Chem. A 4, 15788–15822.
Tian, H., Xu, B., Chen, H., Johansson, E.M.J., Boschloo, G., 2014. Solid-state perovskite-sensitized p-type mesoporous nickel oxide solar cells. ChemSusChem 7, 2150–2153.
Tvingstedt, K., Malinkiewicz, O., Baumann, A., Deibel, C., Snaith, H.J., Dyakonov, V., Bolink, H.J., 2014. Radiative efficiency of lead iodide based perovskite solar cells. Sci. Rep. 4, 6071.
Tyagi, M., Tomar, M., Gupta, V., 2012. Influence of hole mobility on the response characteristics of p-type nickel oxide thin film based glucose biosensor. Anal. Chim. Acta 726, 93–101.
Wang, Z.K., Gong, X., Li, M., Hu, Y., Wang, J.M., Ma, H., Liao, L. S., 2016. Induced crystallization of perovskites by a perylene underlayer for high-performance solar cells. ACS Nano 10, 5479–5489.
Wang, Y., Rho, W.-Y., Yang, H.-Y., Mahmoudi, T., Seo, S., Lee, D.-H., Hahn, Y.-B., 2016. Air-stable, hole-conductor-free high photocurrent perovskite solar cells with CH3NH3PbI3–NiO nanoparticles composite. Nano Energy 27, 535–544.
Wang, K.-C., Shen, P.-S., Li, M.-H., Chen, S., Lin, M.-W., Chen, P., Guo, T.-F., 2014. Low-temperature sputtered nickel oxide compact thin film as effective electron blocking layer for mesoscopic NiO/CH3NH3PbI3 perovskite heterojunction solar cells. ACS Appl. Mater. Interfaces 6, 11851–11858.
Wang, K.-C., Jeng, J.-Y., Shen, P.-S., Chang, Y.-C., Diau, E.W.-G., Tsai, C.-H., Chao, T.-Y., Hsu, H.-C., Lin, P.-Y., Chen, P., Guo, T.-F., Wen, T.-C., 2014. p-type mesoscopic nickel oxide/organometallic perovskite heterojunction solar cells. Sci. Rep. 4, 4756.
Wang, S., Sina, M., Parikh, P., Uekert, T., Shahbazian, B., Devaraj, A., Meng, Y.S., 2016. Role of 4-tert-butylpyridine as a hole transport layer morphological controller in perovskite solar cells. Nano Lett. 16, 5594–5600.
Wang, J.M., Wang, Z.K., Li, M., Hu, K.H., Yang, Y.G., Hu, Y., Gao, X.Y., Liao, L.S., 2017. Small molecule-polymer composite hole-transporting layer for highly efficient and stable perovskite solar cells. ACS Appl. Mater. Interfaces 9, 13240–13246.
Wang, J.-M., Wang, Z.-K., Li, M., Zhang, C.-C., Jiang, L.-L., Hu, K.-H., Ye, Q.-Q., Liao, L.-S., 2018. Doped copper phthalocyanine via an aqueous solution process for normal and inverted perovskite solar cells. Adv. Energy Mater. 8, 1701688.
Wei, Z., Chen, H., Yan, K., Yang, S., 2014. Inkjet printing and instant chemical transformation of a CH3NH3PbI3/nanocarbon electrode and interface for planar perovskite solar cells. Angew. Chem. 126, 13455–13459.
Wei, H., Xiao, J., Yang, Y., Lv, S., Shi, J., Xu, X., Dong, J., Luo, Y., Li, D., Meng, Q., 2015. Free-standing flexible carbon electrode for highly efficient hole-conductor-free perovskite solar cells. Carbon 93, 861–868.
Wei, Z., Yan, K., Chen, H., Yi, Y., Zhang, T., Long, X., Li, J., Zhang, L., Wang, J., Yang, S., 2014. Cost-efficient clamping solar cells using candle soot for hole extraction from ambipolar perovskites. Energy Environ. Sci. 7, 3326–3333.
Wei, Z., Chen, H., Yan, K., Zheng, X., Yang, S., 2015. Hysteresis-free multi-walled carbon nanotube-based perovskite solar cells with a high fill factor. J. Mater. Chem. A 3, 24226–24231.
Wu, H., Wang, L.-S., 1997. A study of nickel monoxide (NiO), nickel dioxide (ONiO), and Ni(O 2) complex by anion photoelectron spectroscopy. J. Chem. Phys. 16.
Xiao, J., Shi, J., Liu, H., Xu, Y., Lv, S., Luo, Y., Li, D., Meng, Q., Li, Y., 2015. Efficient CH3NH3PbI3 perovskite solar cells based on graphdiyne (GD)-modified P3HT hole-transporting material. Adv. Energy Mater. 5. 1401943-n/a.
Xu, X., Liu, Z., Zuo, Z., Zhang, M., Zhao, Z., Shen, Y., Zhou, H., Chen, Q., Yang, Y., Wang, M., 2015. Hole selective NiO contact for efficient perovskite solar cells with carbon electrode. Nano Lett. 15, 2402–2408.
Xu, Q., Wang, F., Tan, Z.A., Li, L., Li, S., Hou, X., Sun, G., Tu, X., Hou, J., Li, Y., 2013. High-performance polymer solar cells with solution-processed and environmentally friendly CuO x anode buffer layer. ACS Appl. Mater. Interfaces 5, 10658–10664.
Xu, B., Zhang, J., Hua, Y., Liu, P., Wang, L., Ruan, C., Li, Y., Boschloo, G., Johansson, E.M.J., Kloo, L., Hagfeldt, A., Jen, A.K. Y., Sun, L., 2017. Tailor-making low-cost spiro[fluorene-9,9′-xanthene]-based 3D oligomers for perovskite solar cells. Chem 2, 676–687.
Yan, W., Ye, S., Li, Y., Sun, W., Rao, H., Liu, Z., Bian, Z., Huang, C., 2016. Hole-transporting materials in inverted planar perovskite solar cells. Adv. Energy Mater. 6. 1600474-n/a.
Yang, L., Cai, F., Yan, Y., Li, J., Liu, D., Pearson, A.J., Wang, T., 2017. Conjugated small molecule for efficient hole transport in high-performance p-i-n type perovskite solar cells. Adv. Funct. Mater. 27, 1702613.
Yang, Y., Xiao, J., Wei, H., Zhu, L., Li, D., Luo, Y., Wu, H., Meng, Q., 2014. An all-carbon counter electrode for highly efficient hole-conductor-free organo-metal perovskite solar cells. RSC Adv. 4, 52825–52830.

Please cite this article in press as: Pitchaiya, S. et al., A review on the classification of organic/inorganic/carbonaceous hole transporting materials for perovskite solar cell application. Arabian Journal of Chemistry (2018), https://doi.org/10.1016/j.arabjc.2018.06.006

Yao, K., Li, F., He, Q., Wang, X., Jiang, Y., Huang, H., Jen, A.K.Y., 2017. A copper-doped nickel oxide bilayer for enhancing efficiency and stability of hysteresis-free inverted mesoporous perovskite solar cells. Nano Energy 40, 155–162.

Ye, S., Sun, W., Li, Y., Yan, W., Peng, H., Bian, Z., Liu, Z., Huang, C., 2015. CuSCN-based inverted planar perovskite solar cell with an average PCE of 15.6%. Nano Lett. 15, 3723–3728.

Yeo, J.-S., Kang, R., Lee, S., Jeon, Y.-J., Myoung, N., Lee, C.-L., Kim, D.-Y., Yun, J.-M., Seo, Y.-H., Kim, S.-S., Na, S.-I., 2015. Highly efficient and stable planar perovskite solar cells with reduced graphene oxide nanosheets as electrode interlayer. Nano Energy 12, 96–104.

Yin, X., Yao, Z., Luo, Q., Dai, X., Zhou, Y., Zhang, Y., Zhou, Y., Luo, S., Li, J., Wang, N., Lin, H., 2017. High efficiency inverted planar perovskite solar cells with solution-processed NiOx hole contact. ACS Appl. Mater. Interfaces 9, 2439–2448.

Yixin Zhao, A.M.N., Zhu, Kai, 2014. Effective hole extraction using MoOx-Al contact in perovskite CH3NH3PbI3 solar cells. Appl. Phys. Lett. 104.

You, J., Hong, Z., Yang, Y., Chen, Q., Cai, M., Song, T.-B., Chen, C.-C., Lu, S., Liu, Y., Zhou, H., Yang, Y., 2014. Low-temperature solution-processed perovskite solar cells with high efficiency and flexibility. ACS Nano 8, 1674–1680.

You, J., Meng, L., Song, T.-B., Guo, T.-F., Yang, Y., Chang, W.-H., Hong, Z., Chen, H., Zhou, H., Chen, Q., Liu, Y., De Marco, N., Yang, Y., 2015. Improved air stability of perovskite solar cells via solution-processed metal oxide transport layers. Nat. Nanotechnol. 11, 75.

Yu, Z., Liu, W., Fu, W., Zhang, Z., Yang, W., Wang, S., Li, H., Xu, M., Chen, H., 2016. An aqueous solution-processed CuOX film as an anode buffer layer for efficient and stable organic solar cells. J. Mater. Chem. A 4, 5130–5136.

Zhang, Y., Elawad, M., Yu, Z., Jiang, X., Lai, J., Sun, L., 2016. Enhanced performance of perovskite solar cells with P3HT hole-transporting materials via molecular p-type doping. RSC Adv. 6, 108888–108895.

Zhang, L., Liu, T., Liu, L., Hu, M., Yang, Y., Mei, A., Han, H., 2015. The effect of carbon counter electrodes on fully printable mesoscopic perovskite solar cells. J. Mater. Chem. A 3, 9165–9170.

Zhang, H., Wang, H., Chen, W., Jen, A.K.Y., 2017. CuGaO2: a promising inorganic hole-transporting material for highly efficient and stable perovskite solar cells. Adv. Mater. 29. 1604984-n/a.

Zhang, F., Yang, X., Cheng, M., Wang, W., Sun, L., 2016. Boosting the efficiency and the stability of low cost perovskite solar cells by using CuPc nanorods as hole transport material and carbon as counter electrode. Nano Energy 20, 108–116.

Zhao, R.M.K., Yan, B., Yang, Y., Kim, T., Amassian, A., 2015. Solution-processed inorganic copper(I) thiocyanate (CuSCN) hole transporting layers for efficient p–i–n perovskite solar cells. J. Mater. Chem. A 3, 20554–20559.

Zheng, D., Yang, G., Zheng, Y., Fan, P., Ji, R., Huang, J., Zhang, W., Yu, J., 2017. Carbon nano-onions as a functional dopant to modify hole transporting layers for improving stability and performance of planar perovskite solar cells. Electrochim. Acta 247, 548–557.

Zhou, Z., Li, X., Cai, M., Xie, F., Wu, Y., Lan, Z., Yang, X., Qiang, Y., Islam, A., Han, L., 2017. Stable inverted planar perovskite solar cells with low-temperature-processed hole-transport bilayer. Adv. Energy Mater. 7. 1700763-n/a.

Zhou, H., Shi, Y., Dong, Q., Zhang, H., Xing, Y., Wang, K., Du, Y., Ma, T., 2014. Hole-conductor-free, metal-electrode-free TiO2/CH3NH3PbI3 heterojunction solar cells based on a low-temperature carbon electrode. J. Phys. Chem. Lett. 5, 3241–3246.

Zhu, Z., Bai, Y., Zhang, T., Liu, Z., Long, X., Wei, Z., Wang, Z., Zhang, L., Wang, J., Yan, F., Yang, S., 2014. High-performance hole-extraction layer of Sol–Gel-processed NiO nanocrystals for inverted planar perovskite solar cells. Angew. Chem. 126, 12779–12783.

Zhu, L., Shao, G., Luo, J.K., 2011. Numerical study of metal oxide heterojunction solar cells. Semicond. Sci. Technol. 26, 085026.

Zhu, Z., Zhao, D., Chueh, C.-C., Shi, X., Li, Z., Jen, A.K.Y., 2018. Highly efficient and stable perovskite solar cells enabled by all-crosslinked charge-transporting layers. Joule 2, 168–183.

Zimmermann, I., Urieta-Mora, J., Gratia, P., Aragó, J., Grancini, G., Molina-Ontoria, A., Ortí, E., Martín, N., Nazeeruddin, M.K., 2017. High-efficiency perovskite solar cells using molecularly engineered, thiophene-rich, hole-transporting materials: influence of alkyl chain length on power conversion efficiency. Adv. Energy Mater. 7. 1601674-n/a.

Zuo, C., Ding, L., 2015. Solution-processed Cu2O and CuO as hole transport materials for efficient perovskite solar cells. Small 11, 5528–5532.

Please cite this article in press as: Pitchaiya, S. et al., A review on the classification of organic/inorganic/carbonaceous hole transporting materials for perovskite solar cell application. Arabian Journal of Chemistry (2018), https://doi.org/10.1016/j.arabjc.2018.06.006